Tellus SERIES B CHEMICAL AND PHYSICAL METEOROLOGY
PUBLISHED BY THE INTERNATIONAL METEOROLOGICAL INSTITUTE IN STOCKHOLM

Future changes in the Baltic Sea acid–base (pH) and oxygen balances

By ANDERS OMSTEDT[1]*, MOA EDMAN[1], BJÖRN CLAREMAR[2], PETER FRODIN[3], ERIK GUSTAFSSON[4], CHRISTOPH HUMBORG[4], HANNA HÄGG[4], MAGNUS MÖRTH[4], ANNA RUTGERSSON[2], GUY SCHURGERS[3], BENJAMIN SMITH[3], TERESIA WÄLLSTEDT[4] and ALLA YUROVA[5], *[1]Department of Earth Sciences, University of Gothenburg, Gothenburg, Sweden; [2]Department of Earth Sciences, Uppsala University, Uppsala, Sweden; [3]Department of Physical Geography and Ecosystem Science, Lund University, Lund, Sweden; [4]Baltic Nest Institute, Stockholm University, Stockholm, Sweden; [5]Hydrometeorological Centre of Russia, Moscow, Russia*

(Manuscript received 21 August 2012; in final form 18 November 2012)

ABSTRACT

Possible future changes in Baltic Sea acid–base (pH) and oxygen balances were studied using a catchment–sea coupled model system and numerical experiments based on meteorological and hydrological forcing datasets and scenarios. By using objective statistical methods, climate runs for present climate conditions were examined and evaluated using Baltic Sea modelling. The results indicate that increased nutrient loads will not inhibit future Baltic Sea acidification; instead, the seasonal pH cycle will be amplified by increased biological production and mineralization. All examined scenarios indicate future acidification of the whole Baltic Sea that is insensitive to the chosen global climate model. The main factor controlling the direction and magnitude of future pH changes is atmospheric CO_2 concentration (i.e. emissions). Climate change and land-derived changes (e.g. nutrient loads) affect acidification mainly by altering the seasonal cycle and deep-water conditions. Apart from decreasing pH, we also project a decreased saturation state of calcium carbonate, decreased respiration index and increasing hypoxic area – all factors that will threaten the marine ecosystem. We demonstrate that substantial reductions in fossil-fuel burning are needed to minimise the coming pH decrease and that substantial reductions in nutrient loads are needed to reduce the coming increase in hypoxic and anoxic waters.

Keywords: *Ocean acidification, marine acidification, eutrophication, climate change, Baltic Sea, Kattegat*

1. Introduction

Coastal seas, such as the Baltic Sea (Fig. 1), link the continents to the ocean by means of fresh water and matter fluxes. The coupling is complex and illustrates the interconnection between human activity and physical, chemical and biological processes in whole drainage basin. This can be exemplified by the spread of anoxic bottom water in coastal seas, which is closely linked to both riverine nutrient load and stagnation periods (e.g. Hansson and Gustafsson, 2011). Changes due to deoxygenation, marine acidification and climate change may have severe implications for carbon and nutrient cycles, as well as for marine ecosystems. Both the CO_2 and O_2 dynamics are central to these changes and crucial to marine biogeochemical cycles.

Climate change may increase the temperature and decrease oxygen concentrations, and it could also increase acidification (Doney et al., 2009) and enlarge nutrient loads due to increased river runoff (Meier et al., 2011). Eutrophication may increase biological primary production, thereby increasing the pH (Omstedt et al., 2009; Borges and Gypsens, 2010) or possibly increasing the acidification in subsurface coastal waters due to mineralization (Cai et al., 2011). Eutrophication may also increase the extent of anoxic deep waters (Diaz and Rosenberg, 2008), which would increase the total alkalinity and thus the buffer effect (Ulfsbo et al., 2011; Edman and Omstedt, 2013). In addition, plankton growth and mineralization strongly influence acidification, compounding the direct effect of rising atmospheric CO_2 concentrations with a possible indirect, climate-driven effect. The relative importance of the factors influencing acidification may be difficult to disentangle as variability often is large (Wootton et al., 2008).

*Corresponding author.
email: Anders.Omstedt@gvc.gu.se

Citation: Tellus B 2012, **64**, 19586, http://dx.doi.org/10.3402/tellusb.v64i0.19586

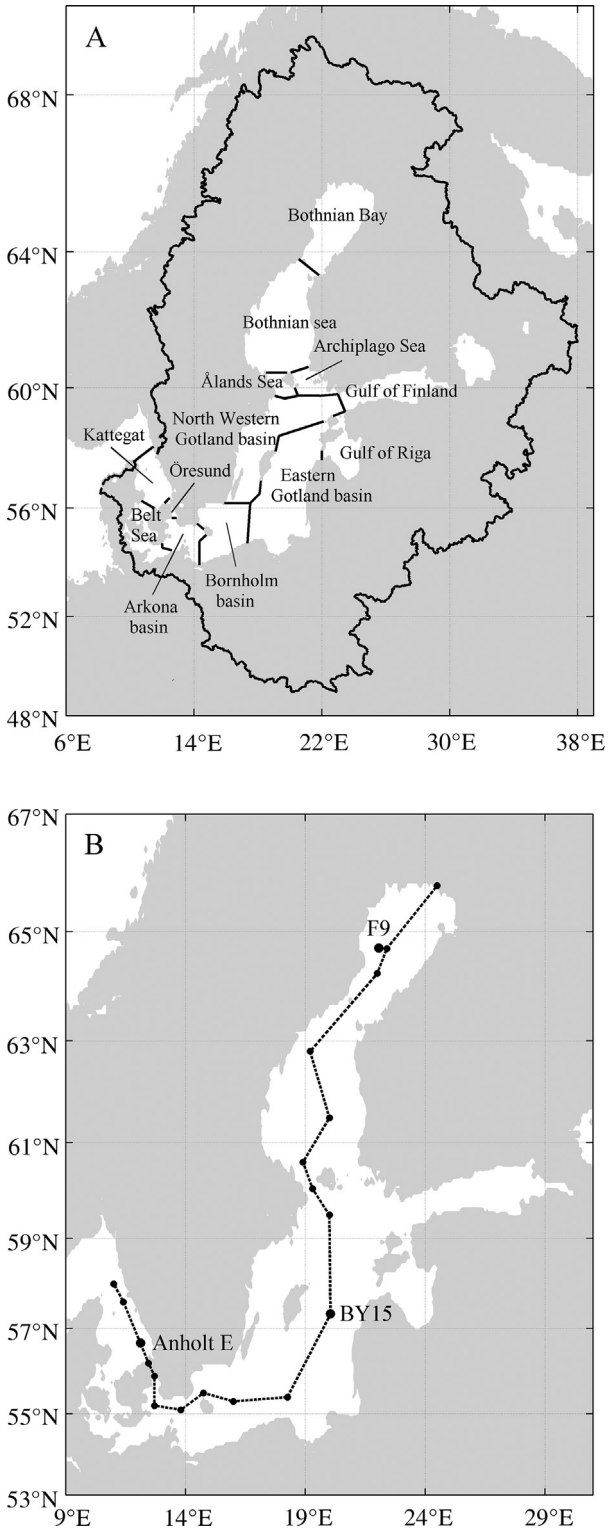

Fig. 1. a) Map of the Baltic Sea showing the drainage basin and PROBE-Baltic sub-basins. b) Map of the Baltic Sea showing the transect path (dashed line), and the three validation stations (larger dots).

Coastal upwelling regions with high biological production may be particularly exposed to the effects of climate change due to the upwelling of acidic and nutrient-rich deep water (e.g. Feely et al., 2008; Gruber et al., 2012).

The carbon cycle encompasses the fluxes of carbon dioxide (CO_2) between the atmosphere and water, and the flux of organic and inorganic carbon (C_{org} and C_T) and carbonate (represented by total alkalinity, A_T) from rivers into the marine environment. Significant amounts of C_{org} originate from land and are mediated by biological and biogeochemical processes occurring in vegetation and soils (Humborg et al., 2004; Kulinski and Pempkoviak, 2011, 2012). Added to these fluxes are the fluxes between water and sediment and between coastal seas and open ocean. The oxygen (O_2) and nutrient cycles are closely coupled through primary production and mineralization in the water body, and the different carbon components are of various origins. The largest pool of carbon is in the form of total inorganic carbon in deep waters. This is because of the effective transport mechanisms of plankton taking up CO_2 in the euphotic zone and leaving the zone as sinking particles. This exported organic material is mineralized on its way to the sea floor and, particularly in the shallow Baltic Sea, at the sediment–water interface (Schneider et al., 2010). Added to this is carbon exported from the drainage basin, which is estimated to be the largest carbon flow into the Baltic Sea (Kulinski and Pempkowiak, 2011). The second largest source of carbon in the Baltic Sea is believed to be the inflow, mainly of inorganic carbon, from the North Sea. Only a small fraction of all the carbon entering the Baltic Sea ends up in the sediments, and the largest part returns to the water column. Approximately 60% of the river-transported carbon of terrestrial origin in the Baltic Basin is in the form of inorganic carbon while the rest is organic (Kulinski and Pempkowiak, 2012), creating oversaturation when entering the Baltic Sea (Humborg et al., 2009).

The lands surrounding and draining into the Baltic Sea cover an area some four times larger than the Baltic itself and encompass a diversity of climate zones and landscapes. A broad distinction can be made between the continental parts, characterised by a cultivated landscape and a temperate climate, and the Fennoscandian boreal region, dominated by evergreen forests of native conifers, in many areas interspersed with wetlands. The Baltic Sea thus receives significant river runoff from the surrounding land, and this catchment runoff is a major source of biogenic elements such as carbon, nitrogen and phosphorous. Earlier studies indicate, for example, that a major part of the organic carbon found in the Baltic Sea water column is of terrestrial origin, over 60% in the Baltic Proper and up to almost 90% in the Bothnian Bay

(Alling et al., 2008). Carbon is exported from the catchment in the form of dissolved organic carbon (C_{org}^{terr}) as well as dissolved inorganic carbon (C_T^{terr}) in the form of bicarbonate (HCO_3^-), carbonate (CO_3^{2-}) and gaseous CO_2. In river systems, bicarbonate and carbonate originate from the weathering of silicate and carbonate minerals, and C_{org}^{terr}, in particular, originates from forest soils and wetlands. Important factors governing the size and seasonality of this flux include the accumulation and decay rate of soil organic matter and the flushing of the organic horizon in conjunction with rain, snowmelt and flooding. These factors are in turn strongly influenced by variations in climate. C_{org}^{terr} loads from individual catchments have moreover been found to differ markedly depending on land use and vegetation cover (Humborg et al., 2004).

The marine carbon system has been introduced into some Baltic Sea model studies (Leinweber et al., 2005; Kuznetsov et al., 2008; Omstedt et al., 2009, 2010; Gustafsson, 2012; Edman and Omstedt, 2013). Kuznetsov et al. (2008) and Leinweber et al. (2005) have focused on the modelling of nitrogen fixation during plankton blooms. Omstedt et al. (2009) used a coupled basin model, i.e. the PROBE-Baltic model, to analyse the uptake and release of CO_2 in surface water. This Baltic Sea model was used in a sensitivity study of acidification together with box modelling and CO_2 calculations (Omstedt et al., 2010). By extending the biological modelling in PROBE-Baltic, Gustafsson (2012) analysed hypoxia and various management options for nutrient loads to the Baltic Sea. The model was further expanded by Edman and Omstedt (2013), who included CO_2–O_2 dynamics for both anoxic and oxic conditions.

Most coupled hydrological–biogeochemical models addressing the Baltic Sea catchment have dealt with nutrient fluxes and eutrophication issues. Mörth et al. (2007) developed a conventional hydrological model, i.e. the Catchment Simulation Model (CSIM), describing nutrient fluxes to all major basins of the Baltic Sea, simultaneously simulating 117 major watersheds based on the generalised watershed loading function (GWLF) model approach. In the present work, we have developed the CSIM model by simultaneously simulating nutrient, C_T^{terr}, C_{org}^{terr} and alkalinity (A_T^{terr}) concentrations and fluxes from all major watersheds within the Baltic Sea drainage area. In such a large-scale approach, it is crucial to handle water fluxes consistently in hydrological simulations and to have loading functions that facilitate comparison of riverine transport between Baltic Sea sub-basins that differ substantially. Deposition data regarding major anions and cations were used to estimate weathering rates for silicate and carbonate minerals for each watershed. Landscape data and C_{org}^{terr} production values for each land cover class were estimated using a dynamic vegetation-ecosystem model, LPJ-GUESS (Smith et al., 2001), forced by gridded monthly data on temperature, precipitation, incoming solar radiation and atmospheric CO_2 concentration. LPJ-GUESS simulates the potential natural vegetation in dynamic equilibrium with the long-term climate for each simulated locality (grid cell). Net primary production (NPP), estimated annually, governs the growth of plants, while plant mortality and biomass turnover (shedding of leaves and fine roots) augments soil carbon via additions of fresh litter. Decomposition of litter and two soil carbon pools provides the substrate for microbial C_{org}^{terr} production, the export of which beyond the vegetation root zone depends on water flow within the soil profile and sorption of C_{org}^{terr} to soil particles. A further description of LPJ-GUESS and its set-up for this study is provided in Appendix A.1.1. C_{org}^{terr} fluxes and a dynamically computed fractional coverage of the land cover types, broadleaved forest, evergreen forest, open land (cropland or grassland) and non-vegetated land (for areal weighting of the fluxes) were passed to the CSIM hydrochemistry model in order to compute the C_{org}^{terr} export at the catchment level.

The new CSIM model (Appendix A.1.2) was able to conduct numerous scenario analyses of river runoff (Q_r), A_T^{terr}, C_T^{terr} and C_{org}^{terr} river loads to the Baltic Sea as functions of land cover change and to analyse changes in river discharge as a function of regional climate change. Besides the CSIM model, we applied a regression model that uses runoff and human population size to make scenario estimates of the yearly nutrient load from the various Baltic Sea sub-basins. This regression model is based on the models used by Smith et al. (2005) and Hägg et al. (2010).

Increased atmospheric greenhouse gases are expected to increase the temperature, which will in turn affect other atmospheric parameters. Several parameters, particularly concerning the water cycle, are subject to great uncertainty. Using simulations from various global climate models (GCMs) forced by a number of emission scenarios and downscaled by a regional climate model (RCM), we have modelled a range of possible atmospheric forcings of the Baltic Sea region (Fig. 2). The regional climate data together with land-use change scenarios based on common socio-economic assumptions were then used to run our system of coupled models encompassing the relevant biogeochemical dynamics of the Baltic Sea, its drainage basin and the river network linking terrestrial and marine systems. To account for the consequences of future changes in land use, we adopted land-use change scenarios consistent with the IPCC-SRES narratives and downscaled to a Europe-wide grid for the EU project ALARM (Spangenberg et al., 2012, Appendix A.2).

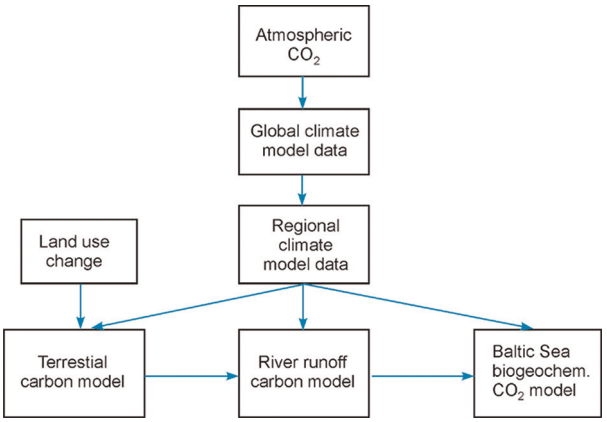

Fig. 2. Sketch of the model system including a terrestrial carbon model (LPJ-Guess forced by land usage change, atmospheric CO_2, temperatures and precipitation and exporting land cover fractions and C_{org}^{terr} to CSIM), river runoff carbon model (CSIM forced by C_{org}^{terr}, temperatures and precipitation and exporting runoff, total nitrogen, total phosphorous, C_{org}^{terr}, C_{T}^{terr} and A_{T}^{terr} to PROBE-Baltic), and a Baltic Sea carbon model (PROBE-Baltic forced by Kattegat sea levels calculated from air pressure, wind, temperature, humidity, total cloudiness, precipitation, atmospheric CO_2, runoff, total nitrogen, total phosphorous, C_{org}^{terr}, C_{T}^{terr} and A_{T}^{terr}). The drainage basin and Baltic Sea models are forced by using global climate models downscaled by one regional climate model.

The present work describes the first integrated Baltic Basin (i.e. Baltic Sea and drainage basin) model framework that addresses both climate change and the carbon and oxygen cycles; the aim is to apply this model framework to address eutrophication, marine acidification and climate change using a large number of available scenarios.

2. Material and methods

2.1. Scenario narratives and selection

A selection of IPCC-SRES narratives (Nakicenovic et al., 2000), together with climate model simulations based on these, was adopted as the basic scenario framework of the present study (see Table 1). Twelve GCM scenarios, downscaled for the Baltic Sea Basin using the RCA3 RCM, were chosen to span the possible future climate development of the 21st-century and to accommodate uncertainty in the nature of the global climate system (represented by three GCMs), natural climate variability (represented by three ensemble members for the ECHAM5 GCM) and the future course of socio-economic development (represented by three GHG emission scenarios). The three first runs in Table 1 represent the three ensemble members for which we use ECHAM A1B in run 1 as our baseline scenario. Run 1, together with runs 4 and 5, includes the three GCM runs

Table 1. Scenario simulations in the present study

Number	GCM	SRES narrative	Ensemble member	Land cover	Nutrient loads	Factor addressed
1, 13*	ECHAM	A1B	#1	Present-day	Present-day	Baseline scenario
2, 14*	ECHAM	A1B	#2	Present-day	Present-day	Natural variability
3, 15*	ECHAM	A1B	#3	Present-day	Present-day	Natural variability
4, 16*	HadCM	A1B		Present-day	Present-day	Climate system
5, 17*	CCSM	A1B		Present-day	Present-day	Climate system
6, 18*	ECHAM	A2		Present-day	Present-day	Emissions (higher)
7, 19*	ECHAM	B1		Present-day	Present-day	Emissions (lower)
8, 20*	ECHAM	A1B	#1	GRAS	Present-day	Land cover change
9, 21*	ECHAM	A1B	#1	Present-day	Medium	Nutrient loads change
10, 22*	ECHAM	A2		BAMBU	Business as usual	Multifactor, business as usual
11, 23*	ECHAM	A1B	#1	GRAS	Medium	Multifactor, balanced policy
12, 24*	ECHAM	B1		SEDG	Baltic Sea action plan	Multifactor, environmental
25	20th-century	A2		20th-century	20th-century	CO_2 emissions (high)
26	20th-century	A1B	#1	20th-century	20th-century	CO_2 emissions (medium)
27	20th-century	B1		20th-century	20th-century	CO_2 emissions (low)
28	20th-century	SC_85		20th-century	20th-century	CO_2 emissions (very high)
29	ECHAM	A2		20th-century	20th-century	Bias-corrected version of scenario 10
30	ECHAM	A1B	#1	20th-century	20th-century	Bias-corrected version of scenario 11
31	ECHAM	B1		20th-century	20th-century	Bias-corrected version of scenario 12

*With bias corrections for air temperature and precipitation.

for A1B emissions. Run 1, together with runs 6 and 7, represents the three emission scenarios in which ECHAM is our core GCM. Runs 8, 9 and 11 represent three runs investigating the land cover and nutrient loads in which we start from ECHAM A1B but change land cover and nutrient loads. Runs 10, 11 and 12 start from ECHAM but use different land cover assumptions and nutrient loads. Run 10 is defined as business as usual with A2 emissions (BAU-A2), run 11 is defined as a medium scenario (medium-A1B) and run 12 is the most optimistic scenario with nutrient loads according to the Baltic Sea Action Plan (BSAP; HELCOM, 2007) and the B1 emission scenario (BSAP-B1). Runs 13–24 follow runs 1–12, respectively, but with bias corrections. To analyse the importance of climate change and the coupling between atmosphere, land and seas, sensitivity studies were also added in runs 25–31 (Table 1).

The decision to use only one RCM was based on a study by Kjellström et al. (2011), who evaluated 16 RCMs forced by seven GCMs for the 1961–1990 period. They found that biases in climate models were strongly related to errors in the large-scale circulations in the GCMs, and that the uncertainty depended largely on choice of GCM. The skills of the climate models used to simulate present climate conditions are briefly summarised in Appendix A.2.

To complement the climate model scenarios and associated CO_2 concentration trajectories, land-use change scenarios based on the same underlying socio-economic assumptions (i.e. the IPCC-SRES narratives) were adopted from the ALARM project (Spangenberg et al., 2012). By land-use change we envisage both land cover transitions (e.g. forest to agriculture) and changes in nutrient loads associated with, for example, agricultural management. Baseline (present-day) land cover was adopted from the Global Land Cover (GLC) database. The classes distinguished for the vegetation modelling were forests, open land (i.e. grasslands and croplands), wetlands and non-vegetated land.

In effect, we investigate three fully consistent, multifactor management options: the first is a 'business-as-usual' scenario based on the IPCC-SRES A2 narrative (BAU-A2), the second is a 'balanced policy' scenario based on the IPCC-SRES A1B narrative (medium-A1B) and the last is an 'environmental policy' scenario combining the BSAP (HELCOM, 2007) with the B1 narrative from IPCC-SRES (BSAP-B1).

2.2. Climate models

2.2.1. GCM data. Meteorological forcing data and scenarios have been extracted from freely available sources (Appendix A.2). Atmospheric scenario data (i.e. temperature and humidity at 2 m, air pressure, wind at 10 m, cloud cover and precipitation) were extracted through the EU project ENSEMBLES (Hewitt and Griggs, 2004; Kjellström et al., 2011, Nikulin et al., 2011) for the Baltic Sea drainage basin and for the various Baltic Sea sub-basins for the 1960–2100 period (some runs 1960–2098). We use data from three coupled atmosphere–ocean GCMs downscaled by one GCM (RCA3) (Kjellström et al., 2005) to a 50×50 km grid. The GCMs used here are ECHAM5 (Jungclaus et al., 2006; Roeckner et al., 2006), HadCM3 (Gordon et al., 2000) and CCSM3 (Collins et al., 2006), forced by the emission scenarios A1B, A2 and B1. To evaluate the present climate, i.e. 1960–2004, downscaled ERA-40 reanalysis (Uppala et al., 2005) was used. All simulations are summarised in Table 1.

The atmospheric deposition data were retrieved from a gridded database with monthly deposition fields for ions of sulphate, nitrate, ammonium and chloride and the base cations sodium, magnesium, potassium and calcium. The database covers the 1960–2006 period and was constructed from simulations of the European Monitoring and Evaluation Programme (EMEP) model (Simpson et al., 2003), interpolated EMEP measurements (Hjellbrekke and Fjæraa, 2007) and emission data from EDGAR-HYDE (Olivier et al., 2001).

The atmospheric carbon dioxide concentration and its time evolution were converted from global to local values using the method of Rutgersson et al. (2009). Scenario concentrations were taken from the IPCC Special Report on Emission Scenarios (Nakicenovic et al., 2000).

2.2.2. Regional downscaling. GCMs have a coarse resolution, so, to better represent a limited region such as the Baltic Sea, the global data were dynamically downscaled by one RCM. As climate models applied on a regional scale have deficits in both their water and heat balances (e.g. Omstedt et al., 2000; BACC Author Team, 2008; Meier et al., 2011), we apply the so-called delta-change bias correction. Correction factors (anomalies) were determined based on the difference between the climate model control simulation and observations, averaged over the 1961–1990 control period. ERA-40 was used for precipitation observations over sea, while gridded observations from E-OBS (Haylock et al., 2008) and the CRU TS 2.1 global historical climate database (New et al., 2000) were used over land. Arithmetic anomalies for temperature and relative anomalies for precipitation were determined for each month and grid cell and applied to all years of the relevant climate model scenario.

2.3. The model system

The model system involves two land surface models, i.e. LPJ-GUESS (Appendix A.1.1) and CSIM (Appendix A.1.2) and one Baltic Sea model, i.e. PROBE-Baltic (Appendix A.1.3). The model design was set up as shown in Fig. 2. All three models are forced by the downscaled climate data according to the chosen scenario narratives. Land cover classes from the GLC baseline land cover database and the ALARM land-use change scenarios were used to force the LPJ-GUESS terrestrial vegetation–ecosystem model.

The LPJ-GUESS terrestrial vegetation–ecosystem model was enhanced for the purpose of this study by incorporating a submodel of C_{org}^{terr} production in organic wetland soils. The model was set up for application across the 50×50 km simulation grid for which climate data were provided. The CSIM Baltic Sea catchment model was expanded by including base cations, anions, C_{org}^{terr} and C_{T}^{terr} (taking into account the outputs of LPJ-GUESS), and now calculates parameters such as river runoff, nutrient load, total alkalinity, pH and pCO_2 for 82 rivers and 35 coastal areas draining into the Baltic Sea. The Baltic Sea model PROBE-Baltic was expanded by including coupled CO_2–O_2 dynamics under both oxic and anoxic conditions according to Edman and Omstedt (2013). The model version used here also includes pelagic and benthic organic carbon and the expanded biological set-up together with detailed description of the full model formulation were presented in Gustafsson (2012).

2.4. Validation of the model system

The projection of the future anthropogenic climate change due to increased greenhouse gas emissions includes many uncertainties. Räisänen (2006) reviews the reliability of climate models based on three considerations: model skill in simulating the present-day climate, inter-model agreement on future climate change, and model ability to simulate climate change that has already occurred. We use the results of the Baltic Sea model for the 1995–2009 period to validate the model system, and then use Baltic Sea modelling as a tool for investigating the integrated physical and biogeochemical effects of using forcing data from climate models. Validation data for the Baltic Sea properties were extracted from the Swedish Meteorological and Hydrological Institute (SMHI) database Svenskt HavsARKiv (SHARK). The A_T and pH data are reliable from 1995 and the measured A_T values have been corrected according to the method presented by Ulfsbo et al. (2011) to account for the oxidation of H_2S during the measurement procedure.

The validation method followed that of Edman and Omstedt (2013), in which two objective quality metrics were applied. The first metric is the coefficient of correlation, r [eq. (1)], between the observed and modelled vertical profiles of various parameters. This skill metric quantifies how well a model returns the correct shape of a distribution.

$$r = \frac{\sum_{i=1}^{n} \left(P_i - \overline{P}\right)\left(O_i - \overline{O}\right)}{\sqrt{\sum_{i=1}^{n} \left(P_i - \overline{P}\right)^2 \sum_{i=1}^{n} \left(O_i - \overline{O}\right)^2}} \quad (1)$$

Here n is the number of observations, O_i the ith of n observations, and P_i the corresponding model value. The averages of observations and model results are indicated by $\overline{O}$ and $\overline{P}$, respectively. A cost function, C [eq. (2)], is used as a second skill metric. It is used to evaluate how well a model returns the magnitude of a parameter, and is a good complement to the correlation coefficient's evaluation of shape.

$$C = \frac{\sum_{i=1}^{n} \left| \frac{P_i - O_i}{SD(O_i)} \right|}{n} \quad (2)$$

The cost function normalises the bias between the model results (P_i) and observed data (O_i) by the standard deviation (SD) of the observations. When applied to the mean depth profiles, the averaging of eq. (2) is volume weighted. We follow Eilola et al. (2009) and interpret values of 0–1 as indicating good agreement between model and observations, 1–2 as reasonable agreement, and anything above 2 as poor agreement. Both skill metrics are dimensionless and have been presented graphically at the three validation sites for seven key physical and biogeochemical parameters.

2.5. Environmental indicators

The reaction of CO_2 with seawater reduces the availability of the carbon ions necessary for calcium carbonate ($CaCO_3$) skeleton and shell formation. The extent to which organisms are affected depends on the $CaCO_3$ saturation state (Ω), a saturation of 1.0 indicating that the solid face of the calcium carbonate in question is in equilibrium with the dissolved components. The saturation state of calcite and aragonite in seawater can be calculated from:

$$\Omega = \frac{\left[CO_3^{2-}\right]\left[Ca^{2+}\right]}{K_{C/A}} \quad (3)$$

where $K_{C/A}$ is the solubility product for either calcite or aragonite. Calcium carbonate is almost under saturated in

winter in the Baltic Sea, which may explain the absence of coccolithophorids (Tyrell et al., 2008).

Brewer and Peltzer (2009) introduced the respiration index (RI) as a measure of the physiological limits for marine animals. The index connects O_2 and CO_2 dynamics by means of the following relationship:

$$\mathrm{RI} = \log_{10}\left(\frac{\mathrm{pO_2}}{\mathrm{pCO_2}}\right) \quad (4)$$

where pO_2 and pCO_2 denote the partial pressure of oxygen and carbon dioxide, respectively. In a marine region with a low RI (<1.0), the low index may be due to low partial pressure of O_2 or to high partial pressure of CO_2, as in hypoxic or anoxic areas. Reductions below 1 in the RI may be taken to indicate an increased threat to marine life. We also add hypoxic area as an indicator of severe consequences for marine life, and define it as area with an oxygen level below 2 mg of O_2 L^{-1} (or approximately 90 μmol O_2 kg^{-1}) and for example benthic organisms are strongly affected by oxygen concentrations less than this threshold (Conley et al., 2002).

3. Results and discussion

3.1. Climate change

The uncertainties in climate models relate to many factors (Räisänen, 2006; IPCC, 2007; BACC Author Team, 2008) that greatly affect the heat balance and water cycle. All simulations indicate a warming trend (of the order of 3–5°C in annual temperature by 2100, see Appendix A.2) and the variation in annual warming among the models is of the order of 1–2°C.

The scenario data indicate that the whole drainage basin may become wetter in annual average terms, particularly in the eastern part; winters are expected to be either more or less wetter than the annual average by the end of the 21st-century, most significantly in the A2 scenario. Bear in mind that there are too few simulation members to estimate the true variability.

3.2. Land surface and drainage basin

The present-day calculated total alkalinities for rivers were generally lower than the alkalinity input used in the marine model for the present-day situation, particularly in the Kattegat (offset almost 90%) and the southern Baltic Sea (offset about 40%). The rivers' A_T^{terr} values were therefore increased by constant values, giving total alkalinities for river runoff in accordance with Hjalmarsson et al. (2008).

Averaged across the drainage basin, the LPJ-GUESS model simulated local C_{org}^{terr} fluxes of 9.0 gC m^{-2} yr^{-1} under present (1961–1990) climate and land-use conditions, with the highest mean fluxes originating from areas north of approximately 60°N, characterised by boreal forests and wetlands. Wetlands were simulated to have the highest C_{org}^{terr} production on an area basis, yielding an average concentration of 128 mg of C L^{-1}. These values may be compared with the constants of 40 and 8 mg of C L^{-1} assumed for forests and open land, respectively, which correspond to typical or average C_{org}^{terr} runoff concentrations for temperate forest landscapes, based on two literature syntheses (Michalzik et al., 2001; Borken et al., 2011). C_{org}^{terr} fluxes, modelled by LPJ-GUESS, increased in all future scenarios, by 30–43% depending on the scenario. Increased temperatures and a resultant increase in vegetation activity and net ecosystem production, increasing both the available substrate and rate of decomposition of plant biomass-derived organic matter, provided the most important explanation for the increase in C_{org}^{terr} exports.

In the scenario calculations of the riverine fluxes, A_T^{terr}, C_T^{terr} and C_{org}^{terr} generally increased, especially in the northern catchments, where the increases were in the range of 20–50%, with the largest increase in the Gulf of Finland (see Fig. 3). The increasing fluxes resulted mainly from the increasing runoff, since modelled concentration changes were relatively small ($<10\%$). In addition, the model suggested increasing fluxes for the Kattegat while no significant flux changes were projected in the Baltic Proper. For the Danish Straits, only the modelled A_T^{terr} increase was significant.

In the two northernmost catchments (i.e. the Bothnian Bay and Bothnian Sea), where C_{org}^{terr} is the dominant carbon fraction, the modelled increase in riverine C_{org}^{terr} concentration was greater than the increase in the inorganic fractions. This was especially true for the Bothnian Bay in the A2 scenario, in which the large C_{org}^{terr} increase contributed to a decrease in A_T^{terr} concentration. For the Baltic Proper and Gulf of Riga, where the inorganic fractions dominate the C_{org}^{terr} fractions, A_T^{terr} concentration increased more than did the C_{org}^{terr} concentration. The modelled scenarios suggest no decreasing riverine fluxes and very few decreasing concentrations.

3.3. Statistical evaluation of the Baltic Sea model for present climate conditions

The Baltic Sea model is validated for present climate conditions by examining its ability to return realistic mean profiles for seven key physical and biogeochemical parameters of the Baltic Sea of today. The forcing data are based on gridded reanalysed weather data and represent the currently best available information. The evaluation is carried out for three validation sites in the Baltic Sea

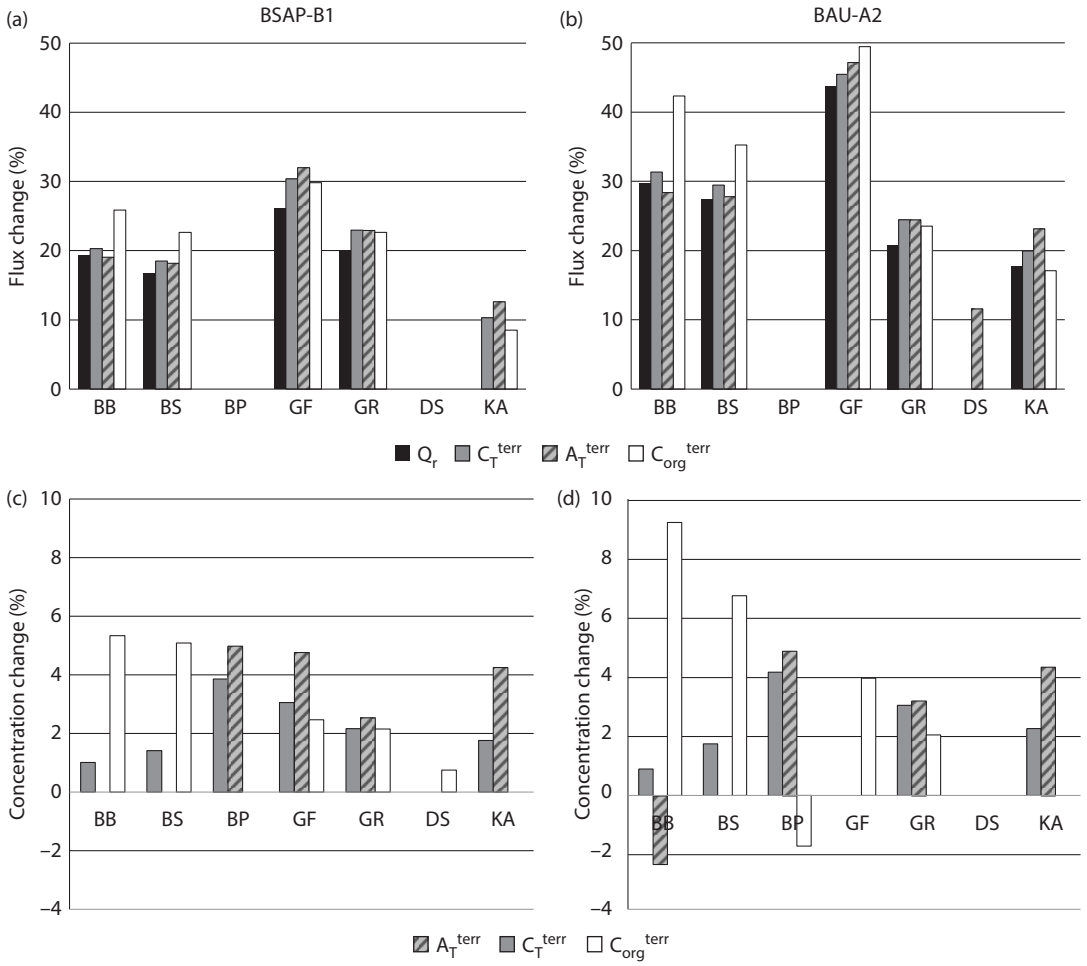

Fig. 3. Modelled trends in runoff (Q_r) as well as (a, b) changes in fluxes and (c, d) concentrations of A_T^{terr}, C_T^{terr} and C_{org}^{terr} over 100 yr according to the BSAP-B1 (a, c) and BAU-A2 (b, d) scenarios. Percent change compared to present day (1996–2005); only significant changes ($p < 0.05$, Mann–Kendall test) are shown. The Baltic Sea sub-basins are denoted: Bothnian Bay (BB), Bothnian Sea (BS), Baltic Proper (BP), Gulf of Finland (GF), Gulf of Riga (GR), Danish Straits (DS), and Kattegat (KA).

(Fig. 1): the Anholt East (Anholt E) station in the Kattegat, the Gotland Deep (BY15) station in the Eastern Gotland Basin and station F9 in the Bothnian Bay. The evaluated parameters are temperature (T), salinity (S), oxygen (O_2), phosphate (PO_4), nitrate (NO_3), total alkalinity (A_T) and pH. The simulated present climate conditions cover the 1958–2009 period, but as measured pH data become reliable only after 1993 and A_T data after 1995, only the 1995–2009 period is considered.

The results of the statistical evaluation are presented in Fig. 4, in which each of the seven parameters is reduced to one point at each validation site. The positions of the points in the diagram indicate how well the parameter is modelled. Lines divide each plot into three fields. The inner field indicates good agreement and strong correlation between the modelled and observed profiles. The middle field indicates that the parameter is acceptably modelled and moderate correlation between the modelled and observed profiles. Parameters in the outer field are poorly modelled.

The evaluation indicates that all parameters were well modelled in the Kattegat and that six of the parameters were well modelled, while nitrate was acceptably modelled, at station BY15 in the Baltic Proper. In the Bothnian Bay, at station F9, only temperature and total alkalinity were well modelled, while salinity and pH were acceptably modelled; however, three of the parameters, i.e. oxygen, phosphate and nitrate, were poorly modelled at this site.

From calculating the mean of all parameters in each basin (Fig. 4, coloured dots), we find that the overall results were good in the Kattegat and Baltic Proper and reasonable in the Bothnian Bay. The Baltic Sea model thus can return the Baltic Sea's current physical and biogeochemical state quit realistic when forced by gridded meteorological data based on observations.

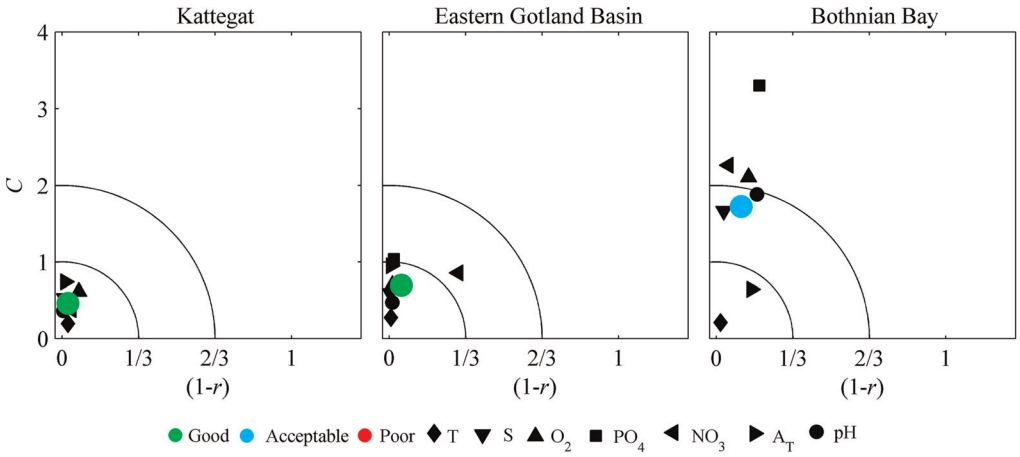

Fig. 4. Statistical evaluation of the reference case (1995–2009) where gridded reanalysed weather data are used as forcing. The Kattegat, Eastern Gotland Basin and Bothnian Bay are represented by observations from Anholt East, BY15 and F9, respectively. The evaluated parameters are temperature (T), salinity (S), oxygen (O_2), phosphate (PO_4), nitrate (NO_3), total alkalinity (A_T) and pH, as indicated in the figure legends. The coloured circles indicate a mean based on all parameters. Calculated parameters inside the inner and outer circles are classified as good and acceptable, respectively; parameters outside the outer circle are classified as poor.

3.4. Statistical evaluation of climate forcing under present climate conditions

To evaluate the model set-up and climate forcing, we examine the model's skill to simulate the present-day climate by comparing the reference case (gridded data were used to force the model, see section *3.3*) with runs where different climate model runs were used as forcing data. The climate forcing control period used is a 30-yr period between 1971 and 2000 that is assumed to represent the present-day climate, and we examine runs with and without bias corrections.

Figure 5 presents the evaluation by plotting the mean values of the seven evaluation parameters (i.e. T, S, O_2, PO_4, NO_3, A_T and pH). The parameter means in all three basins need to be good or acceptable, so the run will be excluded if one basin is poorly simulated. It is clear from the figure that scenario runs 1–12 cannot be used due to the unacceptable parameter modelling, mainly because the observed water balance is not reproduced. However, using the delta-change method improved the simulation output, and the statistical evaluation indicated good to acceptable results for runs 13–31. We will therefore consider only these runs in the following.

3.5. Model system sensitivity and forcing response in the Baltic Sea

This section evaluates the sensitivity of the acidification signal in the results, and seeks to understand which aspects of the climate forcing most strongly influence acidification. Figure 6 shows pH results for three Baltic Sea locations where the differences between two 30-yr periods (1971–2000 and 2069–2098) are evaluated. The reason for using the latter 30-yr periods is due to the fact that some of the climate runs stopped at 2098. The results of each run are presented as three bars: summer (S) and winter (W) mean pH change for the surface water (upper 5 m) and whole year deep water (D) mean pH change (from halocline to bottom). All results indicate a 2–6% decrease in pH throughout the system corresponding to a typical pH reduction of 0.2–0.5 pH units, the only exception being Kattegat deep water, which is strongly influenced by the ocean model boundary condition set as a constant value and should be ignored.

Figure 6 focuses on the uncertainties caused by different initial conditions (ensemble members, runs 13–15) and the use of different GCMs (runs 13, 16 and 17). The forcing is according to the IPCC-SRES A1B narrative and present-day land surface conditions. The Baltic Sea model sensitivity to the different GCMs and their initial conditions is generally one order of magnitude lower than the actual changes and the results are thus mainly insensitive to the studied climate forcing scenarios, the highest sensitivity being found in the central Baltic Sea. The GCM initial conditions and the particular GCM used seem therefore not to be of major importance when calculating future changes in pH.

Figure 7 focuses on the Baltic Sea model response to increased complexity of scenario forcing. Initially, only the atmospheric CO_2 concentrations are according to a scenario narrative (A1B), while replicas of present-day forcing are used for the climate, river and land model components (run 26). We then add complexity to the

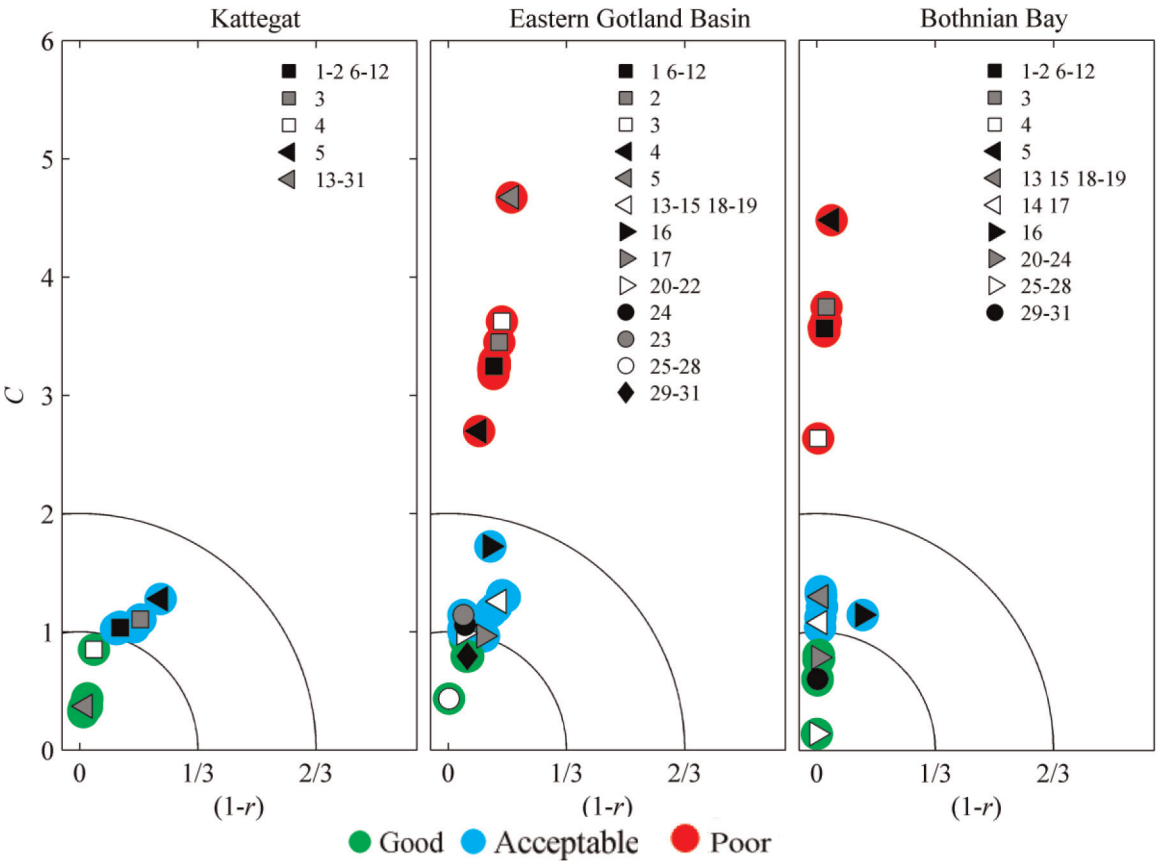

Fig. 5. Statistical evaluation of the climate control case (1971–2000) where different climate model runs are used as forcing data and compared with the reference case. The figure illustrates the statistical mean based on seven different parameters (see Fig. 4). The various climate runs are indicated by their run numbers in the figure (see Table 1). Calculated parameters inside the inner and outer circles are classified as good and acceptable, respectively; parameters outside the outer circle are classified as poor.

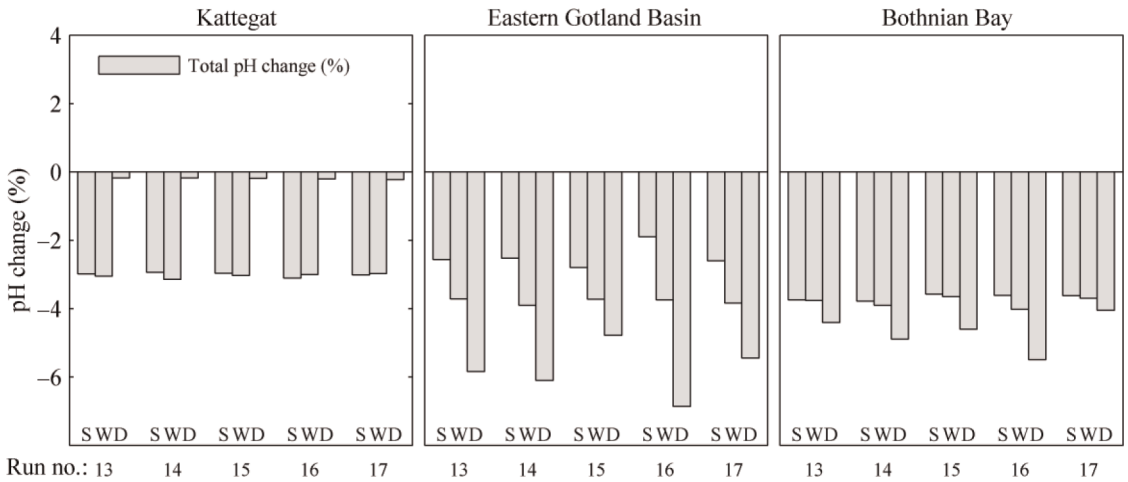

Fig. 6. The Baltic Sea model sensitivity in pH with regard to climate model set-up, comparing 30-yr means from 1971–2000 and 2069–2098. The total pH change is shown in relation to present pH (means for 1971–2000). S and W indicate summer and winter surface means (upper 5 m), respectively, and D indicates depth water mean (from halocline to bottom).

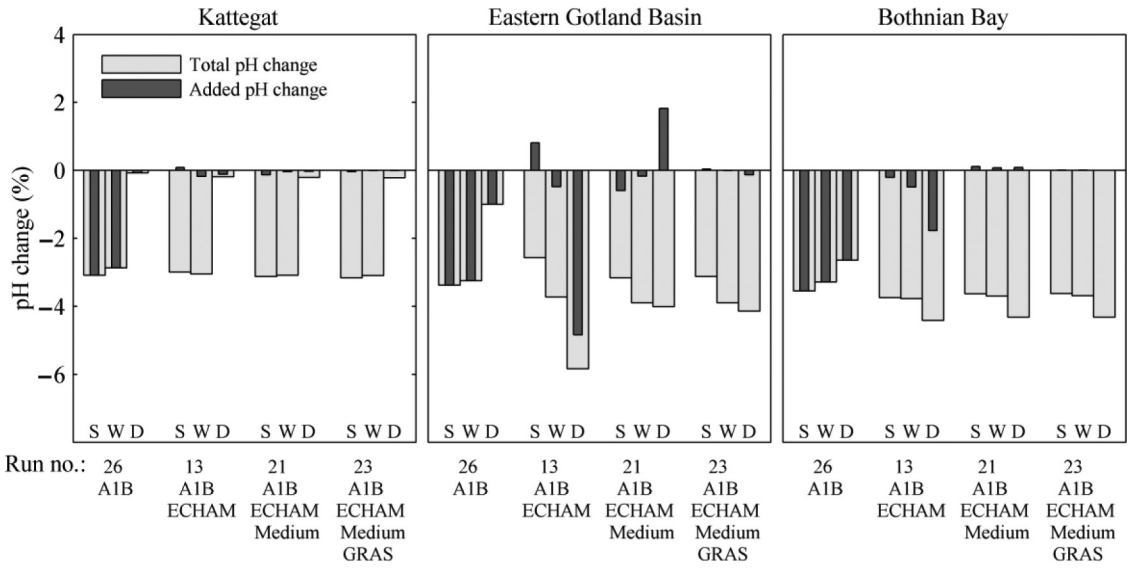

Fig. 7. The Baltic Sea model's pH response to different forcing components, comparing 30-yr means from 1971–2000 and 2069–2098. The added pH change is the deviation from the total pH change that is caused by the added forcing. S and W indicate summer and winter surface means (upper 5 m), respectively, and D indicates depth water mean (from halocline to bottom).

scenario forcing by adding climate change from ECHAM (run 13), river runoff scenarios from CSIM (run 21) and land cover scenarios (run 23). This enables us to recognise the added pH change (dark grey bars) caused by adding each forcing component. The general magnitude and direction of the pH change is immediately set by assuming increased CO_2 emissions (run 26), making atmospheric CO_2 concentrations the main force determining future acidification in the Baltic Sea region. Adding the climate change scenario (run 13) results in some modifications of the surface pH changes, especially in the Baltic Proper where the bias between summer and winter change is increased. The main effect of adding climate change effects, however, is a general decrease in deep-water pH, and winter surface water pH, that is evident in all three basins. The pH drop is indirectly caused by a general sea water temperature increase of 2–3°C, which affects the biogeochemical rates, and especially increases the rate of mineralization. Increased mineralization rates cause more CO_2 to be released to the water, with acidification as the result. The effect is most pronounced in the periodically stagnant bottom water in the Eastern Gotland Basin where the released CO_2 can accumulate. Adding a scenario narrative to the river runoff (run 21) counteracts the effects of climate change in the Baltic Proper, but has minor effects in the other basins. Adding scenario-based land-use changes (run 23) has a minor effect in all three basins.

The main factor controlling the water pH is clearly the atmospheric CO_2 emissions. The results are in good agreement with those of Omstedt et al. (2010), who demonstrated that climate change within currently estimated temperature (several degrees) and salinity (several salinity units) ranges will only marginally change the acid–base (pH) balance.

3.6. *Management options*

The response to climate change and changes in nutrient loads for two alternative story lines representing poor and good management is discussed in this section. The two scenarios considered are defined as the business-as-usual (BAU-A2, run 22) and the BSAP (BSAP-B1, run 24) scenarios, coupled with two atmospheric CO_2 emission scenarios, the A2 and the B1 scenarios, respectively, i.e. our worst-case and best-case scenarios. The BAU-A2 scenario assumes increasing nutrient loads as a result of increasing water runoff and increasing consumption of animal protein and that the atmospheric CO_2 emissions will increase the pCO_2 in the atmosphere up to 850 ppm, slightly more than double present values. The BSAP-B1 scenario introduces substantial reductions in the nutrient load due to generally decreasing population size and future technological improvements, such as more efficient wastewater treatment. Added to this, we have assumed that atmospheric CO_2 emissions will increase the pCO_2 up to only 550 ppm. The latter scenario thus represents an optimistic story line based on the successful management of both global CO_2 emissions and regional nutrient loads.

3.6.1. Transient acidification and hypoxic area. Figure 8 shows the surface water pH in the Eastern Gotland Basin

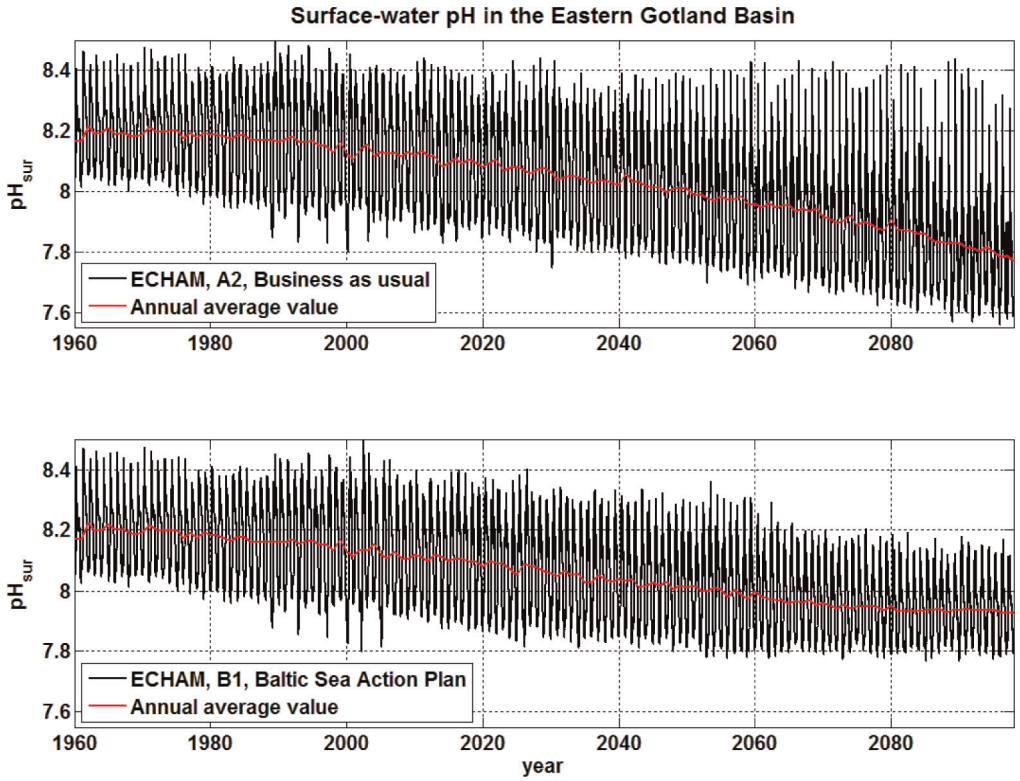

Fig. 8. Daily pH calculations for the Eastern Gotland Basin surface water according to the BAU-A2 and BSAP-B1 projections.

with daily resolution for the two scenarios. The annual averages indicate a declining pH for both runs. For BAU-A2, the seasonal pH cycle is amplified due to an increased nutrient load, which causes the increased biological uptake of CO_2 in surface waters, while this is not the case in the BSAP-B1 narrative. For BSAP-B1, the amplitude is instead reduced after 2060 due to nutrient reductions in this story line. The BSAP-B1 narrative also causes acidification to dampen at the end of the period, which closely relates to the B1 atmospheric CO_2 emission scenario.

The annual dynamics of pH in the Eastern Gotland Basin and of the hypoxic area in the Baltic Proper are shown in Fig. 9. The surface water pH is reduced in both scenarios, which behave similarly until 2060, when BSAP-B1 levels out while BAU-A2 continues to decrease. In the deep water, BAU-A2 causes a continuous decrease throughout the 1960–2100 period, while the BSAP-B1 bottom-water pH already levels out in the first half of the 21st-century.

The calculated hypoxic area increases in both scenarios up to 2040, at which time the BSAP-B1 starts to return to conditions equivalent to those of 1980, while the BAU-A2 hypoxic area continues to increase considerably up to about 2060, at which point it levels out.

Acidification is dampened earlier in the deep waters than in surface waters in the BSAP-B1 scenario. The lower amplitude in Fig. 8 and the smaller hypoxic area in Fig. 9 indicate a biogeochemical system with lower organic biomass production and lower oxygen demand in sediment and subsurface waters. This implies that less CO_2 will accumulate in stagnant bottom waters, reducing the acidification rate during each stagnation period.

With the BSAP-B1 narrative, the Baltic Sea reaches its peak expanse of hypoxic bottom area in the mid–21st-century, and while the oxygen conditions improve later in the century, the acidification will continue until about 2080. When applying the BAU-A2 narrative, acidification does not abate, but continues beyond the timeframe of this study, though the hypoxic area seems to peak in about year 2060. This is due to the topographic restrictions of the stagnant deep-water volume, which is controlled by the halocline depth with well-ventilated waters above.

Meier et al. (2011) investigated the effects of climate warming on hypoxic conditions in the Baltic Sea using three physical–biogeochemical models. They found that, regardless of the global models and climate scenarios they used, hypoxic and anoxic areas will likely increase, or only slightly decrease, relative to present conditions. The present simulated hypoxic areas are in line with their ensemble means, but start from a slightly higher hypoxic area in the 1960s.

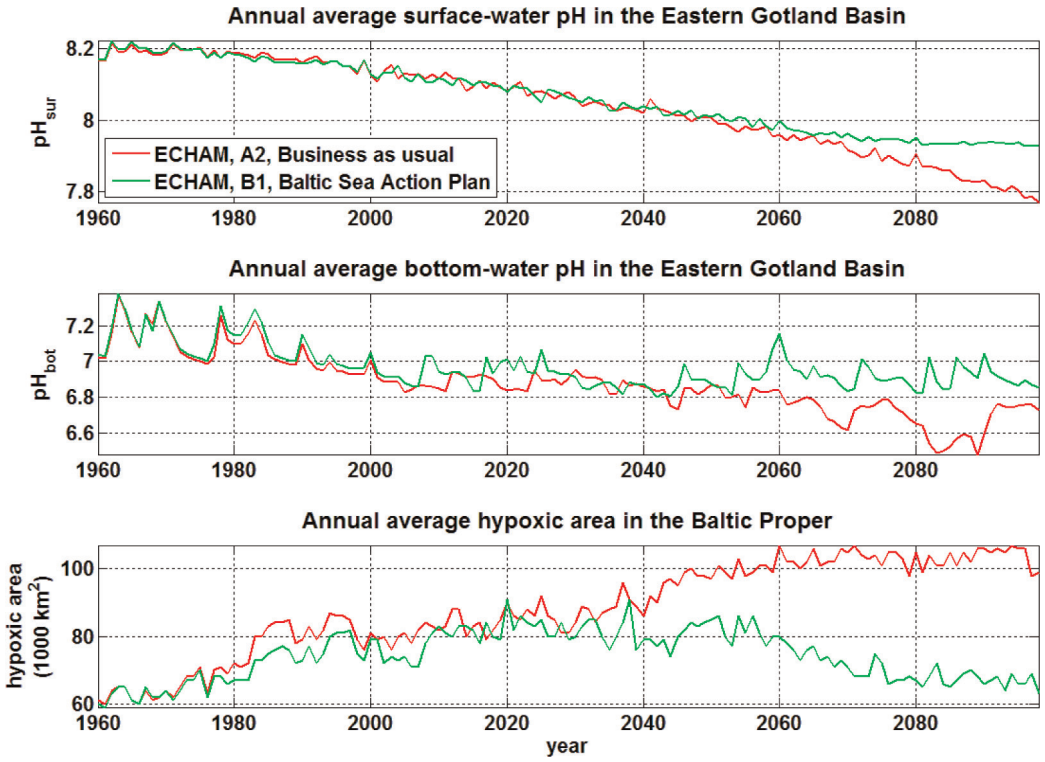

Fig. 9. Annual pH calculations for the Eastern Gotland Basin and hypoxia in the Baltic Proper according to the BAU-A2 and BSAP-B1 projections.

3.6.2. Acidification and oxygen concentrations from the Kattegat to the Bothnian Bay. The scenario response of pH and oxygen concentrations along a longitudinal Baltic Sea transect is examined in Fig. 10 and 11. These figures show the current state and the changes that result from both the BSAP-B1 and BAU-A2 scenario narratives.

Figure 10 shows that acidification will occur over the entire Baltic Sea, no matter which narrative is used. This uniform acidification signals over an area with such varied climatic conditions, and strong biogeochemical gradients, strengthens the proposed conclusion that future pH changes will depend on atmospheric emission load.

Acidification will occur at most depths in both the BSAP-B1 and BAU-A2 scenarios, with the most pronounced pH drops occurring in the surface waters, the Åland Sea deep water, and the intermediate or deep waters of the northern basins. The small pH variation in Kattegat deep water is due to the lateral conditions in the model that assume constant values in the deeper parts of the Kattegat. In both the BSAP-B1 and BAU-A2 scenarios, the Baltic Proper deep water is the least affected by acidification.

The corresponding oxygen concentration results are depicted in Fig. 11. The BSAP-B1 scenario causes only minor changes in the oxygen concentrations in the Baltic Sea as a whole, and with increasing oxygen concentrations in the deeper parts of the Baltic Proper. These increases are caused by lessened hypoxic and anoxic conditions during stagnation periods due to lower nutrient concentrations.

In the BAU-A2 scenario, the most pronounced reductions in oxygen concentration (Fig. 11) occur in the intermediate and deep layers in the Baltic Proper, Åland Sea and Bothnian Sea. In the Baltic Proper, the change is caused by a growing anoxic water volume, which shifts the redox-cline upwards, and an increased oxygen debt in the deepest volume. This is consistent with the increased hypoxic area shown in Fig. 9. The oxygen reductions in the Bothnian Sea will not cause hypoxic conditions, but the volume will be deprived of almost half its oxygen content (-150 μmol kg^{-1}). The model calculations clearly indicate that severe reductions of oxygen will occur if the nutrient loads are not reduced.

The reduced pH decrease in the Baltic Proper bottom-water volume (Fig. 10) is caused by the interaction between the O_2 and CO_2 systems. In the BSAP-B1 case, the bottom-water pH had begun to level out early due to lessened CO_2 deep-water accumulation, caused by the nutrient reductions in the narrative. Continued acidification from CO_2 emissions in BSAP-B1 is then balanced by the recovery of

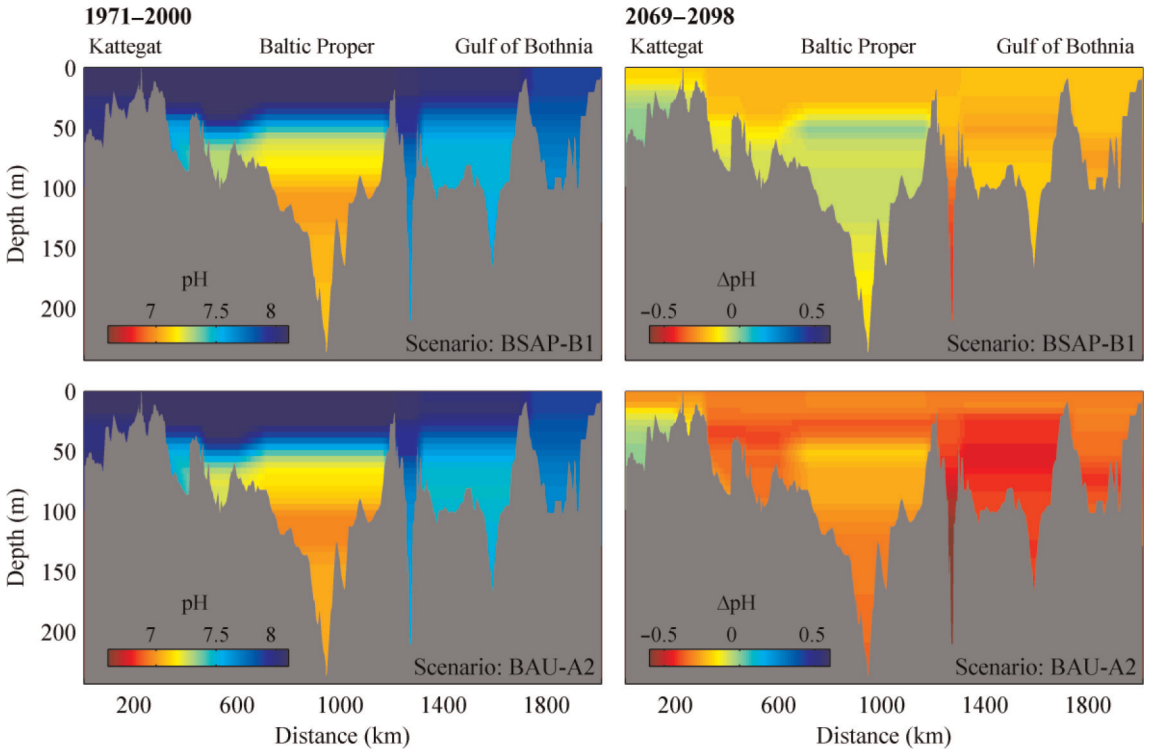

Fig. 10. Current pH (1971–2000) and scenario pH changes (2069–2098) along a Baltic Sea transect (see Fig. 1) for the BSAP-B1 and BAU-A2 scenarios.

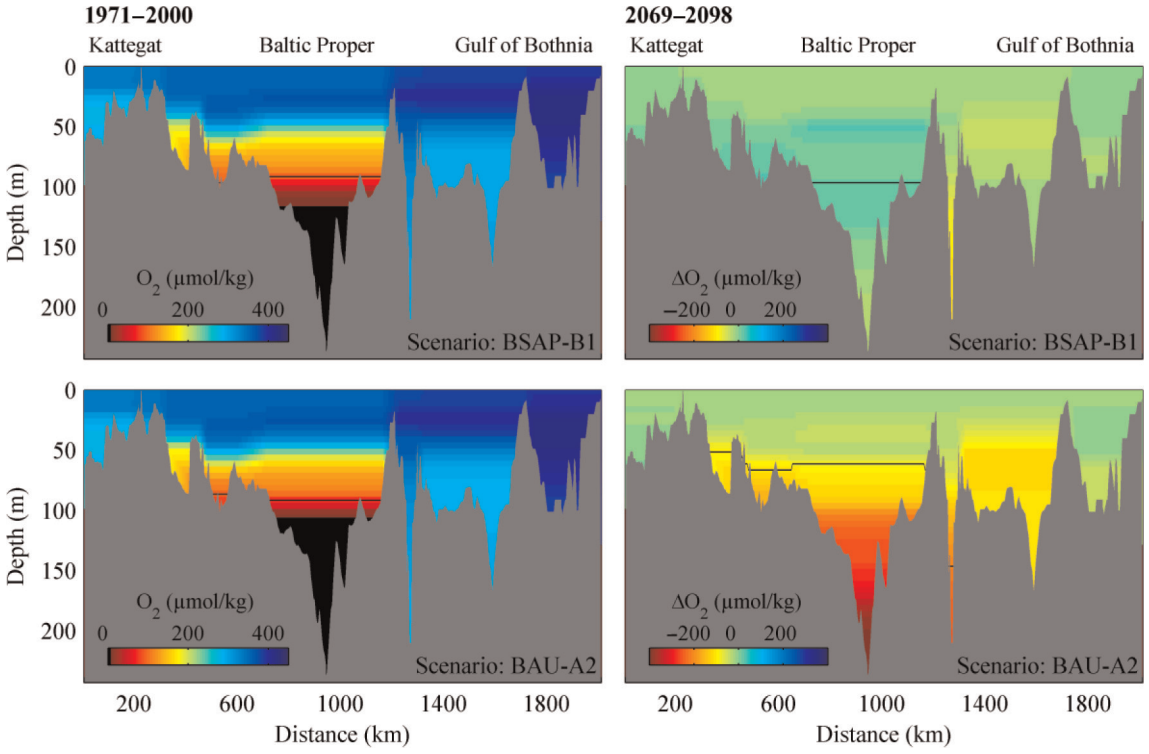

Fig. 11. Current O_2 concentration (μmol kg^{-1}) (1971–2000) and scenario O_2 changes (2069–2098) along a Baltic Sea transect (see Fig. 1) for the BSAP-B1 and BAU-A2 scenarios. The limit for hypoxic water (set as 90 μmol kg^{-1}) is indicated by the black line.

deoxygenated water volumes until the emission signal also levels out. In the BAU-A2 scenario, acidification prevails throughout the modelled period; however, the effect is somewhat counteracted in anoxic bottom waters by alkalinity generation (Edman and Omstedt, 2013), which dampens the effect of increased CO_2 accumulation. The result is net acidification in Baltic Proper bottom water as well in BAU-A2, though the pH decrease is less pronounced than in the surface waters.

3.7. The projected future changes in pH, calcite saturation, RI and hypoxic area

This section considers three fully consistent, multifactor management scenarios defined as BAU-A2, medium-A1B and BSAP-B1 (i.e. runs 22, 23 and 24) and the changes are shown in Fig. 12. We summarise and estimate future changes in pH, but also in Ω, RI, hypoxic and anoxic areas. We seek to quantify these factors because they may stress organisms during the coming century's changes in atmospheric CO_2 levels, nutrient levels and climate. The minor changes in all three parameters in Kattegat deep water are due to the lateral conditions and these should be ignored.

All three indices are reduced throughout the water mass at all three stations. The mean pH drop is 0.2 ± 0.1 throughout the Baltic Sea system. The saturation state of calcite (Ω) will drop to about half the current values in the Baltic Proper and Bothnian Bay. In the Kattegat, the decrease is to about one third of current values (1.1 ± 0.4), but surface waters will remain oversaturated in calcite due to the high current values of approximately 3. In the Baltic Proper, the saturation state is currently close to 1 in winter surface waters, and deep waters are already under saturated. The projected drop in Ω will cause surface waters to become under saturated in winter, and in the Bothnian Bay the values are already below 1. Effectively, calcium carbonate will likely be under saturated in the Baltic Sea in the future, while the Kattegat will remain oversaturated, but to a lesser degree than today.

Today, surface waters and well-ventilated deep-water masses in the Baltic Sea have a RI of approximately 3. According to the calculations, this will decrease by approximately 0.2–0.4 over the coming century, but still remain above 1. For deeper water masses prone to stagnation and deoxygenation, the results for the Baltic Sea deep water shown in Fig. 12 imply large uncertainties, and the development is thus heavily affected by management options. The mean projected change from the BSAP-B1, medium-A1B and BAU-A2 scenarios does, however, indicate a decreased RI, and an increased anoxic and hypoxic bottom area as the most likely future prospect.

4. Summary and conclusions

The Baltic Sea is under strong human pressure and it is critical to understand several complex processes that interact with the ecosystem. Key pressures – such as eutrophication, climate change and marine acidification – influencing the Baltic Sea are recognised, though their impact is far from being understood. Future changes will influence various processes and drivers, including changes in heat, water, nutrient and carbon components that may strongly influence the marine ecosystem.

Observations of the sea constitute the basis of our understanding, and new data regarding, for example, pCO_2, have provided excellent guidance for our modelling activity.

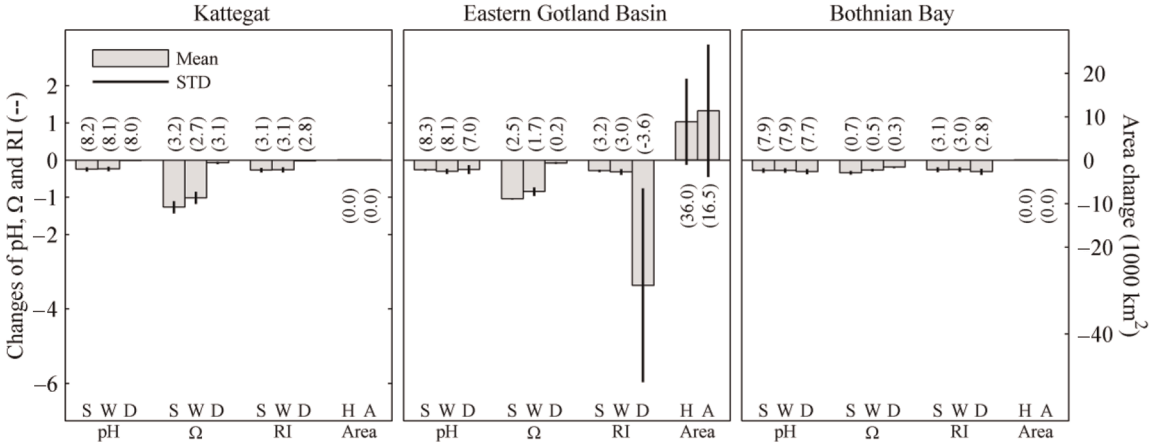

Fig. 12. Mean changes comparing 30-yr means for 1971–2000 and 2069–2098 in environmental indices (pH, Ω, RI, hypoxic (H) and anoxic (A) areas) for the BAU-A2, medium-A1B, and BSAP-B1 narratives. The numbers within parentheses indicate present-day values and *SD* indicates the standard deviation calculated from the three scenarios. S and W indicate summer and winter surface means (upper 5 m), respectively, and D indicates depth water mean (from halocline to bottom).

Monitoring data and long-term well-controlled data series are crucial if we are to manage our sea properly, but management also needs modelling tools if it is to attribute causes to changes or to monitor policy implementation. Acidification in nutrient-rich coastal seas such as the Baltic Sea cannot easily be detected from observations alone; instead, models are needed of both the Sea and its drainage basin. Future monitoring design work needs to involve new instrument components and support model development. To guide the development of the Baltic Sea marine environment in a positive direction, monitoring programmes and design, model tools and development, research programmes and management all need to be much more integrated than they are today. To support such a process, we have developed and applied a new integrated model system based on the cycling of organic carbon and carbon dioxide in the water and the drainage basin of the Baltic Sea, simultaneously addressing eutrophication, climate change and marine acidification.

In the present work, we have examined possible future changes in the Baltic Sea acid–base (pH) and oxygen balances. Based on a model system involving two land surface models (i.e. one terrestrial vegetation–biogeochemistry model and one hydrology–biogeochemistry catchment model) and one Baltic Sea model, a large number of numerical experiments based on forcing datasets and scenarios have been analysed. Using objective statistical methods, we examined the climate runs for present climate conditions. To improve the model's statistical skill, the so-called delta-change method was introduced. Using this method, together with several scenarios and sensitivity studies, the future trajectories of Baltic Sea acidification and oxygen balance were examined. The conclusions of the paper are summarised as follows:

- Increased nutrient load will not inhibit future acidification in the Baltic Sea, but the seasonal pH cycle will become amplified due to increased biological production and mineralization. All examined scenarios indicate future acidification of the whole Baltic Sea.
- The acidification is not sensitive to the choice of GCM or GCM initial conditions, and the main factor controlling the direction and magnitude of future pH changes is the atmospheric CO_2 concentration. Climate change in itself and land-derived changes, such as nutrient load, affect acidification mainly by altering the seasonal cycle and deep-water conditions, but not the direction or general magnitude of the change.
- Apart from decreasing pH, we also project a decreasing saturation state of calcium carbonate, a decreasing RI and increasing hypoxic and anoxic waters, all of which will further threaten the marine ecosystem.
- Substantial reductions in fossil-fuel burning are needed to minimise the coming pH decrease, and substantial reductions in nutrient loads are needed to reduce the coming increase in hypoxic and anoxic water extent.

Reducing potential damage to Baltic Sea ecosystems due to eutrophication, climate change and acidification depends strongly on managing both nutrient loads and CO_2 emissions. However, it seems clear from this study that future eutrophication and acidification are controlled mainly by emission loads (i.e. nutrient loads from land to sea and atmospheric CO_2 emissions). We estimate that hypoxic levels similar to those of the 1980s and acidification of approximately 0.2 ± 0.1 pH units are inevitable, but that management options can strongly influence the actual extent of degradation.

5. Acknowledgements

The work is a part of the BALTEX Phase II and the BONUS + /Baltic-C programmes. Financial support was gratefully received from the University of Gothenburg, the Swedish Research Council (contract no. 621-2007-3750), the European Community's Seventh Framework Programme (FP/2007-2013) under grant agreement no. 217246 made with the joint Baltic Sea research and development programme BONUS, and the Swedish Environmental Protection Agency (contract no. 08/368). Financial support was also received from the European Union EPOCA project (contract no. 211384). We would like to thank Bernd Schneider at Leibniz Institute for Baltic Sea Research for inspiration and support, Stephen Sanborn at Proper English for editing and improving the text, to Erik Kjellström at SMHI for providing climate scenario data and to useful comments from two anonymous reviewers.

6. Appendix

A.1 Models

A.1.1 Baltic Basin vegetation model. Vegetation dynamics and C_{org}^{terr} exports across the Baltic Sea drainage basin were simulated using an adapted version of LPJ-GUESS (Smith et al., 2001), a dynamic vegetation–ecosystem model optimised for regional applications that has been applied to North European ecosystems in numerous studies (e.g. Smith et al., 2001, 2008; Koca et al., 2006; Yurova and Lankreijer, 2007). The version used here incorporates wetland-specific representations of soil hydrology and thermal dynamics based on the model

of Wania et al. (2009), and wetland-specific plant functional types (i.e. mosses, graminoids, and dwarf shrubs) following Wolf et al. (2008).

The model incorporates an adapted version of a C_{org}^{terr} model developed and validated for a wetland catchment in Northern Sweden by Yurova et al. (2008), and this was used to estimate C_{org}^{terr} exports from wetlands, the most important source on an area basis. Wetlands were assumed to be stream-drained, although 'closed-system' wetlands draining only through deep subsurface flow are also common in the Baltic Sea region. The model simulates the production of C_{org}^{terr} in conjunction with microbial decomposition of soil organic matter (SOM). Two SOM pools differing in their resistance to decay, in addition to a litter carbon pool, are represented. Litter resulting from vegetation growth and turnover augment the SOM pools, while temperature and moisture-dependent first-order kinetic functions govern their decay. The sorption and desorption of C_{org}^{terr} onto soil particles is treated as an equilibrium process, dependent on peat bulk density, soil depth and a prescribed partitioning coefficient. The diffusion and transport of C_{org}^{terr} between the upper (acrotelm) and lower soil layers (catotelm) is driven by the concentration difference between the two layers. The water table depth, and thereby the fraction of the soil layer that experiences aerobic conditions, is simulated dynamically for the acrotelm. The catotelm is always water saturated, and assumed to be continuously anaerobic. Runoff export of C_{org}^{terr} is calculated as proportional to the rate of runoff, computed dynamically, from the acrotelm, proportional to the concentration of C_{org}^{terr} there. Stored C_{org}^{terr} is mineralized at a temperature-dependent rate, with a reduced rate applying to the absorbed fraction of C_{org}^{terr}.

For non-wetland areas, C_{org}^{terr} exports were not simulated dynamically, but were estimated based on typical runoff C_{org}^{terr} concentration values of 40 and 8 mg L^{-1} for forests and open land areas, respectively (Michalzik et al., 2001; Borken et al., 2011). Absolute export fluxes of C_{org}^{terr} from these land cover classes depended on ecosystem runoff, simulated dynamically by LPJ-GUESS.

A.1.2. Baltic Basin catchment model. The Catchment Simulation Model (CSIM, Mörth et al., 2007) is a lumped hydrologic model based on the generalised watershed loading function (GWLF; Haith and Shoemaker, 1987). The model was initially developed to simulate stream flow, sediment and nutrient fluxes from mixed-use watersheds in the United States, but was changed in this study to simulate C_T^{terr}, A_T^{terr} and C_{org}^{terr} as well. There are two main sources for carbon in runoff in streams in terrestrial systems, weathering of minerals and C_{org}^{terr} production. Several approaches have been applied to study the weathering regimes of watersheds, ranging from studies of small rivers (White and Blum, 1995) to a more global perspective, studying the geochemistry of very large rivers (Gaillardet et al., 1997; Mortatti and Probst, 2003). These latter large-scale approaches were implemented in the CSIM (Mörth et al., 2007), which estimates the watershed-weathering rates of carbonates and silicates in the major 85 watersheds draining into the Baltic Sea. C_{org}^{terr}, on the other hand, was set to vary according to the increase/decrease in local ecosystem export in the catchment as modelled by LPJ-GUESS (see above).

The model divides each watershed into a number of land-use categories and considers the loads from each category separately. Each land class was set to have a type concentration for each variable (i.e. C_T^{terr}, A_T^{terr} and C_{org}^{terr}) for a reference period (here, the 1997–2000 calibration period). The type concentrations were allowed to change assuming that weathering rates will increase/decrease with yearly mean air temperature in relation to the activation energy for feldspars and calcite. In this study, we used the data from Velbel et al. (1993) and Sjöberg and Rickard (1984), which correspond to an approximately 12% increase (with an activation energy of 77 kJ mol^{-1}) in weathering per degree Celsius for feldspars and 9% (activation energy of 59 kJ mol^{-1}) for calcite. Constant retention was assumed for C_{org}^{terr}, i.e. that a percent increase/decrease in export compared with the reference period was assumed to change the type concentration by the same factor for each land class. C_{org}^{terr} was also assumed to change C_T^{terr} and A_T^{terr}, using a charge density of 9 ueq mg^{-1} based on Hruska et al. (2001).

Runoff and fluxes of C_T^{terr}, A_T^{terr} and C_{org}^{terr} were aggregated to seven Baltic Sea sub-basins: i.e. Bothnian Bay, Bothnian Sea, Baltic Proper, Gulf of Finland, Gulf of Riga, Danish Straits and Kattegat. The significance of trends in the scenarios was analysed using the Mann–Kendall trend test, which is a non-parametric test based on order of observations. The test was suggested by Mann (1945) and has been extensively used with environmental time series (Hipel and McLeod, 1994).

Scenarios of nutrient export from the catchment were modelled by applying a regression model that uses runoff and population size to estimate yearly nutrient loads from the Baltic Sea sub-basins. The regression model is based on the models used in Smith et al. (2005) and Hägg et al. (2010), calibrated for seven sub-basins for the 1970–2000 period and validated using the 2001–2008 period. The yearly loads were then distributed monthly depending on the runoff. The new regression model was used to conduct numerous scenario analyses of the effects of: 1) changing runoff as a result of regional climate change, 2) changes in population size, 3) changes in the consumption of animal

protein, and 4) changes in wastewater treatment efficiency on N and P fluxes from the Baltic Sea catchments.

For the medium and BSAP scenarios (scenarios 9, 11, 12, 21, 23 and 24), the population of each country was allowed to vary according to the UN Medium Population Growth Scenario (United Nations, 2004), while populations were kept steady at present-day levels for the rest of the scenarios. For the business-as-usual (BAU) scenarios (scenarios 10 and 22), we have assumed a linearly increasing consumption of animal protein reaching 75 g per capita and day in 2100 following the approach of Hägg et al. (2010). A level of 75 g of animal protein per capita and day represents medium–high animal protein consumption, on the same order of magnitude as that of many developed countries today. For the rest of the scenarios, the protein consumption was kept at the countries' individual present-day levels. Finally, the BSAP scenario includes an additional decrease in loads corresponding to the reductions that could be expected from future technological improvements (Voss et al., 2011).

A.1.3. Baltic Sea physical–biogeochemical model. For the Baltic Sea, a fully coupled physical–biogeochemical multi-basin model was applied. The model is based on conservation equations in their one-dimensional, time-dependent form and divides the Baltic Sea into 13 natural sub-basins with vertical resolution in each. The coupling between the sub-basins is through strait flow models. The vertical structures are resolved using time-dependent boundary conditions calculated from observed or calculated meteorological conditions, sea levels from the Kattegat, and Baltic Sea river inflow. The physical part of the model includes six equations for momentum (two equations), heat, salinity, turbulent kinetic energy and dissipation of turbulent energy. The chemical part includes six equations for total alkalinity, total inorganic carbon, oxygen, nitrate, total ammonium, and phosphate. The biological part includes three equations for depth- and time-dependent phytoplankton abundance, one equation for zooplankton, and three equations for detritus (C, N and P). The first and third plankton equations treat species that are limited by both nitrogen and phosphorus availability, whereas the second treats species that are able to fix N_2 and thus are limited by phosphorus only. During the scenario runs, the lateral condition associated with sea-level forcing from the North Sea were calculated from the air pressure difference over the Kattegat region (Gustafsson and Andersson, 2001). The lateral condition towards the North Sea also assumed constant properties at the Kattegat deep layers according to observed monthly mean values. As this lateral boundary condition was prescribed far below the Baltic Sea sill depth and the Baltic Sea inflowing water is formed from the Kattegat surface water the boundary condition do not strongly influence the model results inside the Baltic Sea entrance area.

The dissolved CO_2 system is solved from the state variables; total alkalinity (A_T) and total inorganic carbon (C_T). Total inorganic carbon consists of dissolved CO_2 and the products formed by carbonic acid disassociation in water. The speciation is set by interaction with the total acid-base balance of seawater, source and sink terms caused by biogeochemical processes, and air-sea exchange of CO_2. Total alkalinity is a summation of the proton donors and proton acceptors in solution. It thus quantifies the solution's capacity for readjustment of dissolved equilibriums. The variable is affected by riverine input of A_T and source and sink terms caused by biogeochemical processes. Seawater pH and the partial pressure of CO_2 (pCO_2) are determined from the models numerically calculated C_T and A_T. The calculations are initiated by calculating the H^+ concentration through an iterative procedure. To set up the iteration scheme, we follow Dickson et al. (2007) and derive the H^+ concentration from the definition of total alkalinity. When the H^+ concentration is determined, seawater pH and pCO_2 can be calculated from the equilibrium equations.

Monthly C_{org}^{terr} loads to each sub-basin were produced by the LPJ-GUESS terrestrial vegetation–ecosystem model. However, terrestrial dissolved organic carbon, nitrogen and phosphorus are not yet included as individual state variables in the PROBE-Baltic model. Instead, terrestrial organic material is added to the pools of detrital carbon, nitrogen and phosphorus respectively. This is similar to Eilola et al. (2009) and Savchuk et al. (2012) but they only considered nitrogen and phosphorus as they did not consider carbon. As the oxygen consumption is controlled by the availability of biodegradable organic carbon a simulated C_{org}^{terr} load increases, the overall oxygen demand will be enhanced as well. An increased C_{org}^{terr} load will in addition contribute to an increased surface layer pCO_2, and as a result enhanced CO_2 outgassing to the atmosphere (or decreased uptake depending on the direction of the flux).

The full model including information about equations, constants and numerical code is presented in Omstedt (2011) and Gustafsson (2012). The model version is called PROBE-Baltic 3.0 and is freely available on the request from the lead author.

A.2. Scenarios and sensitivity studies

In the present study we have extracted a selection of the IPCC-SRES narratives and climate model simulations to serve as the basic scenarios in the present study. Scenarios A1B, A2 and B1 are used, A1B corresponding to rapid

global economic growth with a mid–21st-century peak in fossil-fuel emissions. Scenario A2 corresponds to a heterogeneous world with slow technological development and continuously increasing fossil-fuel emissions, while scenario B1 corresponds to a convergent world with a focus on global sustainability. Figures B1 and B2 show the response of the various GCMs to the IPCC-SRES narratives for temperature and precipitation. Additional considerations are incorporated relevant to adopting scenarios of land-use change consistent with the underlying socio-economic assumptions of the SRES-based GCM scenarios already chosen. By land-use change we envisage both land cover transitions (e.g. forest to agriculture) and nutrient loads associated with, for example, agricultural management. The primary aim of the future scenario analysis was to explore the dynamics of, and sensitivities, to major forcing factors of the Baltic Sea biogeochemical system in a framework relevant to what we know or may expect in terms of future changes in the drivers. The main criteria for the choice of scenarios to explore were that they cover the scope of possible future changes in a comprehensive way, maintain realistic relationships between different driving variables, and accommodate major aspects of uncertainty.

Land-use change scenarios for the 21st-century consistent with the global narratives underlying the IPCC emission scenarios (Nakicenovic et al., 2000) were adopted from the ALARM project (Spangenberg et al., 2012). The scenarios were modelled using the methodology of Rounsevell et al. (2005, 2006) refined by coupling the European land-use model with a global econometric model that allows estimation of parameters that affect the global population, i.e. global gross domestic product distribution, global trade and markets for land-based commodities (e.g. food and wood products), and with an ecosystem model that computes agricultural yields, accounting for the effects of climate change on crop production. The underlying socio-economic assumptions required by the land-use model were taken from the scenarios developed by the ALARM project (Spangenberg et al., 2012), which in turn may be traced to the IPCC family socio-economic story lines (Nakicenovic et al., 2000). The ALARM scenarios GRAS, SEDG and BAMBU were adopted in combination with climate scenarios forced by the A1B, B1 and A2 emission scenarios, respectively (Table 1). The scenarios provide fractional coverage's of forest, cropland and grassland on a grid-cell basis. They did not extend into Russian territory, and for this part of the Baltic Sea

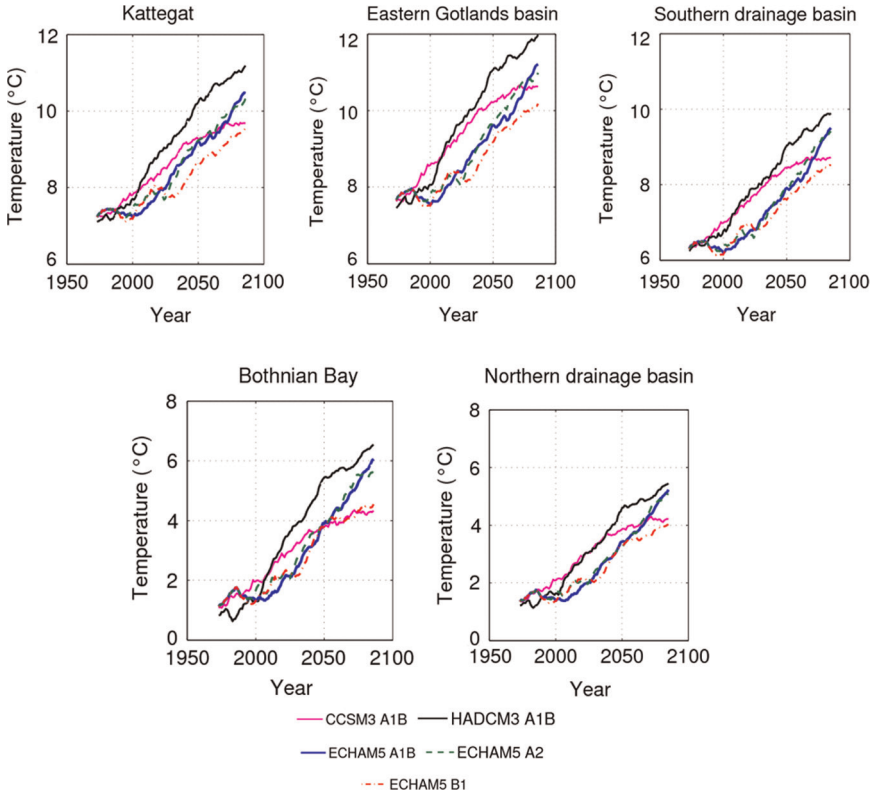

Fig. B1. Trends in bias-corrected temperature (25-yr running mean) for various Baltic Sea sub-basins and scenarios.

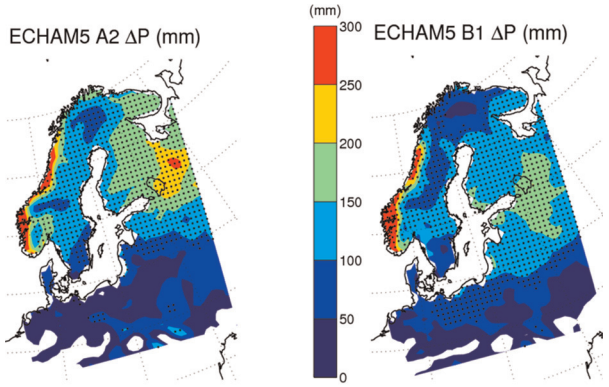

Fig. B2. Simulated difference in mean annual precipitation (2086–2095 minus 1996–2005): (a) scenario A2; (b) scenario B1. Dots indicate areas with positive trends at a significance level above 98%.

catchment area, static, present-day land use was assumed in the future scenarios.

The present approach was based on analysis of an ensemble of simulations (Table 1), each exploring responses to one or a combination of driving factors, i.e. climate, emissions, anthropogenic land cover change and anthropogenic nutrient loads. An additional consideration concerns the inevitable bias all climate models display in representing actual historical climate. The bias was reduced by subtracting the difference (anomaly) between average model simulated values for a given parameter (e.g. temperature) and observations of the same parameter for a control period/simulation from simulated values for a scenario simulation. For precipitation, the relative difference is more useful. This so-called delta-change approach may potentially lead to more 'realistic' simulation of future changes by impact models when driven with bias-corrected climate model output. This has, however, been criticised because the independent correction of bias in different parameters may be expected to break the physical consistency between them. Since there are arguments both supporting and opposing the delta-change approach, it was considered desirable to have simulations driven by both delta-change-corrected and uncorrected climate model output. For temperature, the bias correction was in the range of -6.5 to 5.5°C and for precipitation in the range of -85% to $+130\%$. The largest corrections were associated with the Scandinavian Mountains (mostly outside the drainage basin) for precipitation and, for temperature, with the inner part of Northern Sweden/Finland (warm bias in winter) and the large lakes Ladoga, Onega and Vänern (cold bias in summer). Based on the above considerations, a suite of scenarios was designed with and without delta-change correction and some sensitivity runs (Table 1). The baseline climate/SRES scenario was ECHAM5-A1B- run 1; all other scenarios represent a deviation in terms of one or more factors from this base scenario. Scenario 28 assumes present-day climate conditions in the future as well, but with increasing CO_2 emissions up to 1370 ppm by 2100 in accordance with Moss et al. (2010), representing a worst case that has been applied in the next generation of scenarios for climate change assessment.

Figure B2 shows the change in annual precipitation for the A2 and B1 scenarios over the land areas. The scenarios indicate that the whole drainage basin may become wetter, particularly in the eastern part, and that more or less wetter winters are expected by the end of the 21st-century, most significantly in the A2 scenario.

References

Alling, V., Humborg, C., Mörth, C.-M., Rahm, L. and Pollehne, F. 2008. Tracing terrestial organic matter by δ34S and δ13C signatures in a subarctic estuary. *Limnol. Oceanogr.* **53**(6), 2594–2602.

BACC Author Team. 2008. *Assessment of Climate Change for the Baltic Sea Basin. Series: Regional Climate Studies.* Springer-Verlag, Berlin, & Heidelberg, Germany.

Borges, A. V. and Gypens, N. 2010. Carbonate chemistry in the coastal zone responds more strongly to eutrophication than to ocean acidification. *Limnol. Oceanogr.* **55**, 346–353.

Borken, W., Ahrens, B., Schulz, C. and Zimmermann, L. 2011. Site-to-site variability and temporal trends of DOC concentrations and fluxes in temperate forest soils. *Glob. Chang Biol.* **17**, 2428–2443.

Brewer, P. G. and Peltzer, E. T. 2009. Limits to marine life. *Science.* **324**, 347–348. DOI: 10.1126/science.1170756.

Cai, W.-J., Hu, X., Huang, W.-J., Murrell, M. C., Lehrter, J. C. and co-authors. 2011. Acidification of subsurface coastal waters enhanced by eutrophication. *Nat. Geosci. Lett.* **4**, 766–770. DOI: 10.1038/NGEO1297.

Collins, W. D., Bitz, C. M., Blackmon, M. L., Bonan, G. B. and co-authors. 2006. The community climate system model version 3 (CCSM3). *J. Clim.* **19**, 2122–2143.

Conley, D. J., Humborg, C., Rahm, L., Savchuk, O. P. and Wulff, F. 2002. Hypoxia in the Baltic Sea and basin-scale changes in phosphorus biogeochemistry. *Environ. Sci. Technol.* **36**, 5315–5320.

Diaz, R. J. and Rosenberg, R. 2008. Spreading dead zones and consequences for marine ecosystems. *Science.* **321**, 926.

Dickson, A. G., Sabine, C. L. and Christian, J. R. 2007. Guide to best practices for ocean CO_2 measurements. IOCCP Report, No. 8, Pieces Special Publication 3. Online at: http://cdiac.ornl.gov/ftp/oceans/Handbook_2007/Guide_all_in_one.pdf

Doney, S. C., Fabry, V. J., Feely, R. A. and Kleypas, J. A. 2009. Ocean acidification: the other CO_2 problem. *Annu. Rev. Mar. Sci.* **1**, 169–192. DOI: 10.1146/annurev.marine.010908.163834.

Edman, M. and Omstedt, A. 2013. Modeling the dissolved CO_2 system in the redox environment of the Baltic Sea. *Limnol. Oceanogr.* **58**(1). DOI: 10.4319/lo.2013.58.1.0000.

Eilola, K., Meier, H. E. M. and Almroth, E. 2009. On the dynamics of oxygen, phosphorus and cyanobacteria in the Baltic Sea: a model study. *J. Mar. Syst.* **75**, 163–184.

Feely, R. A., Sabine, C. L., Hernandez-Ayon, J. M., Iansson, D. and Hales, B. 2008. *Science*. **320**(5882), 1490–1492. DOI: 10.1126/science.1155676.

Gaillardet, J., Dupre, B., Allegre, C. J. and Negrel, P. 1997. Chemical and physical denudation in the Amazon river basin. *Chem. Geol.* **142**, 141–173.

Gordon, C., Cooper, C., Senior, C. A., Banks, H., Gregory, J. M. and co-authors. 2000. The simulation of SST, sea ice extent and ocean heat transports in a version of the Hadley Centre coupled model without flux adjustments. *Clim. Dyn.* **16**, 147–168.

Gruber, N., Hauri, C., Lachkar, Z., Loher, D., Frölicher, T. and co-authors. 2012. Rapid progression of ocean acidification in the California current system. *Science*. **337**, 220–223.

Gustafsson, B. and Andersson, H. 2001. Modeling the exchange of the Baltic Sea from the meridional atmospheric pressure difference across the North Sea. *J. Geophys. Res.* **106**(C9), 19731–19744.

Gustafsson E. 2012. Modelling long-term development of hypoxic area and nutrient pools in the Baltic proper. *J. Mar. Syst.* **94**, 120–134. DOI: 10.1016/j.jmarsys.2011.11.012.

Hägg, H. E., Humborg, C., Mörth, C. M., Medina, M. R. and Wulff, F. 2010. Scenario analysis on protein consumption and climate change effects on riverine N export to the Baltic Sea. *Environ. Sci. Technol.* **44**(7), 2379–2385.

Haith, D. A. and Shoemaker, L. L. 1987. Generalized watershed loading functions for streamflow nutrients. *Water Resour. Bull.* **23**, 471–478.

Hansson, D. and Gustafsson, E. 2011. Salinity and hypoxia in the Baltic Sea since A.D. 1500. *J. Geophys. Res.* **116**, C03027. DOI: 10.1029/2010JC006676.

Haylock, M. R., Hofstra N., Klein Tank, A. M. G., Klok, E. J., Jones, P. D. and co-authors. 2008. A European daily high-resolution gridded dataset of surface temperature and precipitation. *J. Geophys. Res. Atmos.* **113**, D20119. DOI: 10.1029/2008JD10201.

Hewitt, C. D. and Griggs, D. J. 2004. Ensemble-based predictions of climate changes and their impacts. *Eos. Trans. AGU.* **85**(52), 566. DOI: 10.1029/2004EO520005.

HELCOM. 2007. *Towards a Baltic Sea Unaffected by Eutrophication. Background document to HELCOM Ministerial Meeting, Krakow, Poland*. Technical Report, Helsinki Comm., Helsinki, Finland.

Hipel, K. W. and McLeod, A. I. 1994. *Time Series Modelling of Water Resources and Environmental Systems*. Elsevier Scientific Publishing Co., Amsterdam, p. 1013.

Hjalmarsson, S., Wesslander, K., Anderson, L. G., Omstedt, A., Perttilä, M. and co-authors. 2008. Distribution, long-term development and mass balance calculation of total alkalinity in the Baltic Sea. *Cont. Shelf. Res.* **28**(4–5), 593–601. DOI: 10.1016/j.csr.2007.11.010.

Hjellbrekke, A.-G. and Fjæraa, A.-M. 2007. *Data Report 2005: Acidifying and Eutrophying Compounds, and Particulate Matter*. EMEP/CCC-Report 1/2007. Norwegian Institute for Air Research, Oslo, Norway.

Hruska, J., Laudon, H., Johsnon, C. E., Köhler, S. and Bishop, K. 2001. Acid/base character of organic acids in a boreal stream during snowmelt. *Water. Resour. Res.* **37**, 1043–1056.

Humborg, C., Mörth, C.-M., Sundbom, M., Borg, H., Blenckner, T. and co-authors. 2009. CO_2 supersaturating along the aquatic conduit in Swedish watersheds as constrained by terrestrial respiration, aquatic respiration and weathering. *Glob. Chang. Biol.* **16**(7), 1966–1978. DOI: 10.1111/j.1365-2486.2009.02092.x.

Humborg, C., Smedberg, E., Blomqvist, S., Mörth, C.-M., Brink, J. and co-authors. 2004. Nutrient variations in boreal and subarctic Swedish rivers: landscape control of land-sea fluxes. *Limnol. Oceanogr.* **49**, 1871–1883.

IPCC. 2007. *Climate Change 2007: The Physical Science Basis. Contribution of Working Group 1 to the Fourth Assessment Report of the Intergovernmental Panel on Climate Change* (eds. S. Solomom, D. Qin, M. Manning, Z. Chen, M. Marquis and co-editors). Cambridge University Press, Cambridge, UK & New York, p. 996.

Jungclaus, J. H., Keenlyside, N., Botzet, M., Haak, H., Luo, J.-J. and co-authors. 2006. Ocean circulation and tropical variability in the coupled model ECHAM5/MPI-OM. *J. Clim.* **19**, 3952–3972.

Kjellström, E., Bärring, L., Gollvik, S., Hansson, U., Jones, C. and co-authors. 2005. A 140-year simulation of European climate with the new version of the Rossby Centre regional atmospheric climate model (RCA3). Reports Meteorology and Climatology, 108, SMHI, SE-60176 Norrköping, Sweden, p. 54.

Kjellström, E., Nikulin, G., Hansson, U., Strandberg, G. and Ullestig, A. 2011. 21st century changes in the European climate: uncertainties derived from an ensemble of regional climate model simulations. *Tellus. A.* **63**, 24–40.

Koca, D., Smith, B. and Sykes, M. T. 2006. Modelling regional climate change effects on Swedish ecosystems. *Clim. Change*. **78**, 381–406.

Kulinski, K. and Pempkowiak, J. 2011. The carbon budget of the Baltic Sea. *Biogeosciences*. **8**, 3219–3230.

Kulinski, K. and Pempkowiak, J. 2012. *Carbon Cycling in the Baltic Sea. GeoPlanet: Earth and Planetary Sciences Series*. Springer-Verlag, Berlin, & Heidelberg, Germany.

Kuznetsov, I., Neumann, T. and Burchard, H. 2008. Model study on the ecosystem impact of a variable C:N:P ratio for cyanobacteria in the Baltic proper. *Ecol. Model.* **219**, 107–114.

Leinweber, A., Neumann, T. and Schneider, B. 2005. The role of N2-fixation to simulate the pCO_2 observations from the Baltic Sea. *Biogeosciences*. **2**, 609–636.

Mann, H. B. 1945. Nonparametric tests against trend. *Econometrica*. **13**(3), 245–259.

Meier, H. E. M., Andersson, H. C., Eilola, K., Gustafsson, B. G., Kuznetsov, I. and co-authors. 2011. Hypoxia in future climates: a model ensemble study for the Baltic Sea. *Geophys. Res. Lett.* **38**, L24608, 6. DOI: 10.1029/2011GL049929.

Michalzik, B., Kalbitz, K., Park, J.-H., Solinger, S. and Matzner, E. 2001. Fluxes and concentrations of dissolved organic carbon and nitrogen: a synthesis for temperate forests. *Biogeochemistry*. **52**, 173–205.

Mortatti, J. and Probst, J. L. 2003. Silicate rock weathering and atmospheric/soil CO_2 uptake in the Amazon basin estimated from river water geochemistry: seasonal and spatial variations. *Chem. Geol.* **197**, 177–196.

Mörth, C.-M., Humborg, C., Eriksson, E., Danielsson, A., Medina, R. and co-authors. 2007. Modeling riverine nutrient transport of the Baltic Sea: a large-scale approach. *Ambio*. **36**, 124–133.

Moss, R. H., Edmonds, J. A., Hibbard, K. A., Manning, M. R., Rose, S. K. and co-authors. 2010. The next generation of scenarios for climate change and assessment. *Nature*. **463**, 747–756. DOI: 10.1038/nature0883.

Nakicenovic, N., Alcamo, J., Davis, G., de Vries, B., Fenhann, J. and co-authors. 2000. Emissions scenarios. *Special Report of Working Group III of the Intergovernmental Panel on Climate Change*. Cambridge University Press, Cambridge, UK, p. 599.

New, M., Hulme, M. and Jones, P. 2000. Representing twentieth-century space–time climate variability. Part II: development of 1901–96 monthly grids of terrestrial surface climate. *J. Clim.* **13**, 2217–2238.

Nikulin, G., Kjellström, E., Hansson, U., Strandberg, G. and Ullerstig, A. 2011. Evaluation and future projections of temperature, precipitation and wind extremes over Europe in an ensemble of regional climate simulations. *Tellus. A*. **63**, 41–55.

Olivier, J. G. J. and Berdowski, J. J. M. 2001. Global emissions sources and sinks. In: *The Climate System* (eds. J. Berdowski, R. Guicherit and B. J. Heij), A.A. Balkema Publishers/Swets & Zeitlinger Publishers, Lisse, The Netherlands, pp. 33–78.

Omstedt, A. 2011. *Guide to process based modelling of lakes and coastal seas*. Springer-Praxis books in Geophysical Sciences. Springer-Verlag, Berlin & Heidelberg, Germany. DOI: 10.1007/978-3-642-17728-6.

Omstedt, A., Edman M., Anderson, L. G. and Laudon, H. 2010. Factors influencing the acid–base (pH) balance in the Baltic Sea: a sensitivity analysis. *Tellus. B*. **62**, 280–295. DOI: 10.1111/j.1600-0889.2010.00463.x.

Omstedt, A., Gustafsson, B., Rodhe, B. and Walin, G. 2000. Use of Baltic Sea modelling to investigate the water and heat cycles in GCM and regional climate models. *Clim. Res.* **15**, 95–108.

Omstedt, A., Gustafsson, E. and Wesslander, K. 2009. Modelling the uptake and release of carbon dioxide in the Baltic Sea surface water. *Cont. Shelf. Res.* **29**, 870–885. DOI: 10.1016/j.csr.2009.01.006.

Räisänen, J. 2006. How reliable are climate models? *Tellus. A*. **59**(1), 2–29. DOI: 10.1111/j.1600-0870.2006.00211.x.

Roeckner, E., Brokopf, R., Esch, M., Giorgetta, M., Hagemann, S. and co-authors. 2006. Sensitivity of simulated climate to horizontal and vertical resolution in the ECHAM5 atmospheric model. *J. Clim.* **19**, 3771–3791.

Rounsevell, M. D. A., Ewert, F., Reginster, I., Leemans, R. and Carter, T. R. 2005. Future scenarios of European agricultural land use II. Projecting changes in cropland and grassland. *Agr. Ecosyst. Environ.* **107**, 117–135.

Rounsevell, M. D. A., Reginster, I., Araújo, M. B., Carter, T. R., Dendoncker, N. and co-authors. 2006. A coherent set of future land use change scenarios for Europe. *Agr. Ecosyst. Environ.* **114**, 57–68.

Rutgersson, A., Norman, M. and Åström, G. 2009. Atmospheric CO_2 variation over the Baltic Sea and the impact on air–sea exchange. *Boreal. Environ. Res.* **14**, 238–249.

Savchuk, O. P., Gustafsson, B. G. and Müller-Karulis, B. 2012. *BALTSEM – A Marine Model for The Decision Support within the Baltic Sea Region*. Technical Report No. 7. BNI Technical Report Series, Stockholm University, Stockholm, Sweden.

Schneider, B., Nausch, G. and Pohl, C. 2010. Mineralization of organic matter and nitrogen transformation in the Gotland Sea deep water. *Mar. Chem.* **119**, 153–161.

Simpson, D., Fagerli, H., Jonson, J. E., Tsyro, S., Wind, P. and co-authors. 2003. Transboundary acidification, eutrophication and ground level ozone in Europe. Pt 1: Unified EMEP model description. EMEP Status Report, 1/2003, Norwegian Meteorological Institute, Oslo, Norway.

Sjöberg, E. L. and Rickard, D. T. 1984. Temperature dependence of calcite dissolution kinetics between 1 and 62°C at pH 2.7 to 8.4 in aqueous solutions. *Geochim. Cosmochim. Acta*. **48**, 485–493.

Smith, B., Knorr, W., Widlowski, J.-L., Pinty, B. and Gobron, N. 2008. Combining remote sensing data with process modelling to monitor boreal conifer forest carbon balances. *For. Ecol. Manage*. **255**, 3985–3994.

Smith, B., Prentice, I. C. and Sykes, M. T. 2001. Representation of vegetation dynamics in modelling of terrestrial ecosystems: comparing two contrasting approaches within European climate space. *Glob. Ecol. Biogeogr.* **10**, 621–637.

Smith, S. V., Swaney, D. P., Buddemeier, R. W., Scarsbrook, M. R., Weatherheadm, M. A. and co-authors. 2005. River nutrient loads and catchment size. *Biogeochemistry*. **75**(1), 83–107.

Spangenberg, J. H., Bondeau, A., Carter, T. R., Fronzek, S., Jaeger, J. and co-authors. 2012. Scenarios for investigating risks to biodiversity. *Glob. Ecol. Biogeogr.* **21**, 5–18.

Tyrell, T., Schneider, B., Charalampopoulou, A. and Riebesell, U. 2008. Coccolithophores and calcite saturation state in the Baltic and Black Seas. *Biogeosciences*. **5**, 485–494.

Ulfsbo, A., Hulth, S. and Anderson, L. G. 2011. pH and biogeochemical processes in the Gotland Basin of the Baltic Sea. *Mar. Chem.* **127**, 20–30.

United Nations. 2004. *World Population to 2300*. Department of Economic and Social Affairs, Population Division, New York.

Uppala, S. M., Kållberg, P. W., Simmons, A. J., Andrae, U., Da Costa Bechtold, V. and co-authors, 2005. The ERA-40 re-analysis. *Q. J. Roy. Meteor. Soc.* **131**, 2961–3012.

Velbel, M. A. 1993. Temperature dependence of silicate weathering in nature: how strong a negative feedback on long-term accumulation of atmospheric CO_2 and global greenhouse warming? *Geology*. **21**, 1059–1062.

Voss, M., Dippner, J. W., Humborg, C., Hurdler, J., Korth, F. and co-authors. 2011. History and scenarios of future development of Baltic Sea eutrophication. *Estuar. Coast. Shelf. Sci.* **92**(3), 307–322.

Wania, R., Ross, I. and Prentice, I. C. 2009. Integrating peatlands and permafrost into a dynamic global vegetation model: 1. Evaluation and sensitivity of physical land surface processes. *Global Biogeochem. Cycles*. **23**, GB3014.

White, A. F. and Blum, A. E. 1995. Effects of climate on chemical weathering in watersheds. *Geochim. Cosmochim. Acta*. **59**(9), 1729–1747.

Wolf, A., Callaghan, T. V. and Larson, K. 2008. Future changes in vegetation and ecosystem function of the Barents Region. *Clim. Change*. **87**, 51–73.

Wootton, T. J., Pfister, C. A. and Forester, J. D. 2008. Dynamic patterns and ecological impacts of declining ocean pH in a high-resolution multi-year dataset. *Proc. Natl. Acad. Sci. U S A*. **105**(48), 18848–18853.

Yurova, A., Sirin, A., Buffam, I., Bishop, K. and Laudon, H. 2008. Modeling the dissolved organic carbon output from a boreal mire using the convection–dispersion equation: importance of representing sorption. *Water. Resour. Res*. **44**, W07411. DOI: 10.1029/2007WR006523.

Yurova, A. Y. and Lankreijer, H. 2007. Carbon storage in the organic layers of boreal forest soils under various moisture conditions: a model study for Northern Sweden sites. *Ecol. Model*. **204**, 475–484.